

000 001 002 003 004 005 006 007 008 009 010 011 012 013 014 015 016 017 018 019 020 021 022 023 024 025 026 027 028 029 030 031 032 033 034 035 036 037 038 039 040 041 042 043 044 045 046 047 048 049 050 051 052 053 THINKING-FREE POLICY INITIALIZATION MAKES DISTILLED REASONING MODELS MORE EFFECTIVE AND EFFICIENT REASONERS

Anonymous authors

Paper under double-blind review

ABSTRACT

Reinforcement Learning with Verifiable Reward (RLVR) effectively solves complex tasks but demands extremely long context lengths during training, leading to substantial computational costs. While multi-stage training can partially mitigate this, starting with overly short contexts often causes irreversible performance degradation, ultimately failing to reduce overall training compute significantly. In this paper, we introduce **Thinking-Free Policy Initialization (TFPI)**, a simple yet effective adaptation to RLVR that bridges long Chain-of-Thought (CoT) distillation and standard RLVR. TFPI employs a simple *ThinkingFree* operation, explicitly discarding the thinking content via a direct `</think>` append, to reduce token usage during inference. Training with *ThinkingFree*-adapted inputs improves performance and lowers token consumption, even in the original slow-thinking mode. Extensive experiments across various benchmarks have shown that TFPI accelerates RL convergence, achieves a higher performance ceiling, and yields more token-efficient reasoning models without specialized rewards or complex training designs. With TFPI only, we train a 4B model to reach 89.0% accuracy on AIM24 and 65.5% on LiveCodeBench using less than 4K H20 hours.

1 INTRODUCTION

Reasoning is a fundamental aspect of human cognition, and equipping artificial intelligence (AI) with strong reasoning capabilities is critical for its deployment and applications (Morris et al., 2023; Huang et al., 2024; Xu et al., 2025c). Progress in pretraining (Shao et al., 2024; Yang et al., 2024; Chen et al., 2025b), supervised fine-tuning (SFT) (Yu et al., 2023; Xu et al., 2024; Tong et al., 2024; Ye et al., 2025; Muennighoff et al., 2025), rigorous evaluation (Rein et al., 2024; Phan et al., 2025; Xu et al., 2025b), reinforcement learning (RL) (Jaech et al., 2024; Guo et al., 2025) has significantly enhanced the reasoning abilities of large language models (LLMs). Among these, RL with verifiable rewards (RLVR) stands out as an effective approach that enables large language models (LLMs) to generate long Chains-of-Thought (CoT) (Wei et al., 2022) spontaneously, and empowers them with unprecedented performance on challenging reasoning tasks. Thus, these RLVR-trained LLMs are termed as long-CoT LLMs, slow-thinking LLMs, or large reasoning models (LRMs).

Compared with initializing from a base LLM, starting from an SFT-distilled LRM typically yields better results and accelerates convergence in RLVR (Guo et al., 2025; An et al., 2025). However, SFT-distilled LRM often produce excessively long responses during the rollout stage of RLVR, which necessitates a large training context length for RLVR. Using such large training contexts also incurs substantial computational costs. A common mitigation strategy is multistage RLVR, which begins with a relatively “short” context and gradually increases the training length (Luo et al., 2025b; An et al., 2025). Nonetheless, Zeng et al. (2025a) argue that multistage training might cause irreversible performance degradation. Moreover, even multistage training demands significant computational resources. For instance, training a 4B model while progressively increasing the maximum context length from 40K to 48K to 52K tokens requires approximately 8K H800 GPU hours (An et al., 2025). These limitations underscore the need for more efficient RLVR training methods.

In this work, we introduce **Thinking-Free Policy Initialization (TFPI)**, a simple yet effective adaptation to RLVR that bridges long Chain-of-Thought (CoT) distillation and standard RLVR. We

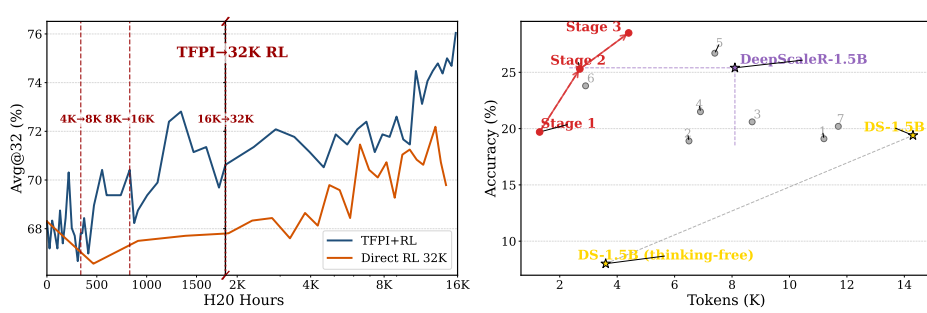


Figure 1: Our proposed TFPI accelerates the convergence of RLVR to a higher performance ceiling (left) and yields more token-efficient reasoning models (right). **Left:** avg@32 versus training compute, measured in H20 hours. “Direct RL” refers to directly training Qwen3–4B with a 32K context window using DAPO, while “TFPI + RL” denotes running 32K-context DAPO after initialization with our 3-stage TFPI. The x-axis for TFPI uses a linear scale during the TFPI phase, followed by a logarithmic scale, with the transition indicated by a black vertical line. **Right:** Average accuracy on 4 reasoning datasets (AIME24/25, Beyond AIME, and GPQA) versus average output tokens. Points in the upper-left region indicate better performance. Baseline names and their corresponding numbers are listed in Table 3. Red dots denote different stages of our TFPI.

first observe that a *ThinkingFree* operation—explicitly discarding the thinking content via a direct `</think>` append—can substantially reduce token usage during inference (Section 3.1). Training with *ThinkingFree*-adapted inputs improves performance and lowers token consumption, even when evaluated in the original slow-thinking mode (Section 3.2). We then formally define TFPI in Section 3.3. As illustrated in Figure 1, TFPI accelerates RL convergence, achieves a higher performance ceiling, and produces more token-efficient LLMs without requiring specialized rewards or complex training designs (Section 4).

Our contributions are as follows: ① We find that *ThinkingFree* can substantially reduce inference costs for distilled LLMs, and that training with *ThinkingFree*-adapted inputs enhances slow-thinking capability. ② We propose TFPI, a fast, low-cost initialization phase for long-CoT RL that accelerates RL convergence and *exhibits transfer* across domains, even when trained solely on mathematics. ③ We show that long-CoT RL following TFPI achieves a higher performance ceiling while producing more token-efficient LLMs without the need for specialized rewards or complex training designs, offering an effective and efficient route to training high-performing LLMs. ④ We provide both behavioral and parameter-level analyses and reveal that TFPI not only preserves the slow-thinking reasoning pattern but also enables substantially faster rollouts in subsequent long-CoT RL stages.

2 PRELIMINARY

Notation. In this paper, we define an LLM parameterized by θ as a policy π_θ . Let x denote a query and \mathcal{D} the set of queries. Given a response y to a query x , its likelihood under the policy π_θ is expressed as $\pi_\theta(y | x) = \prod_{t=1}^{|y|} \pi_\theta(y_t | x, y_{<t})$, where $|y|$ denotes the number of tokens in y . A query-response pair (x, y) is scored by a rule-based outcome reward $r(x, y) \in \{0, 1\}$, indicating whether the response y aligns with the ground truth of x .

RLVR Algorithms. RLVR algorithms are central to the recent success of LLMs, with prominent examples including Proximal Policy Optimization (PPO) (Schulman et al., 2017) and Group Relative Policy Optimization (GRPO) (Shao et al., 2024). PPO constrains updates to remain close to the previous policy $\pi_{\theta_{\text{old}}}$ via clipping. GRPO bypasses the need for the value model by computing relative advantages among responses to the same query. A widely adopted GRPO variant, DAPO (Yu et al., 2025), adds clip-higher, dynamic sampling, and token-level policy-gradient losses to stabilize training. The objective is given by $\mathcal{J}_{\text{DAPO}}(\theta) = \mathbb{E}_{x \sim \mathcal{D}} [\mathcal{J}_{\text{DAPO}}(\theta, x)]$,

$$\mathcal{J}_{\text{DAPO}}(\theta, x) = \left[\frac{1}{\sum_{i=1}^G |y_i|} \sum_{i=1}^G \sum_{t=1}^{|y_i|} \min \left(r_{i,t}(\theta) \hat{A}_{i,t}, \text{clip}(r_{i,t}(\theta), 1 - \varepsilon_{\text{low}}, 1 + \varepsilon_{\text{high}}) \hat{A}_{i,t} \right) \right],$$

s.t. $0 < |\{y_i \mid \text{is_equivalent}(y_i, x)\}| < G$. (1)

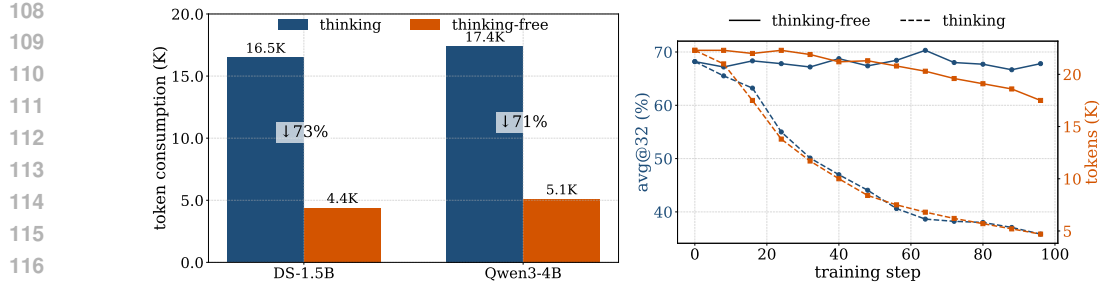


Figure 2: Results of the meta-experiment on the *ThinkingFree* operation. **Left:** Average output tokens in thinking mode and *ThinkingFree* mode on AIME25. **Right:** Evolution of $\text{avg}@32$ and average output tokens on AIME24 with thinking-mode evaluation over training steps **under 4K training response length (both training in thinking mode and *ThinkingFree* mode)**.

Here, $\{y_i\}_{i=1}^G \sim \pi_{\theta_{\text{old}}}(\cdot|x)$ and G is the number of generated responses to each query x (i.e., the group size) and the importance ratio $r_{i,t}(\theta)$ and advantage $\hat{A}_{i,t}$ of token $y_{i,t}$ are:

$$r_{i,t}(\theta) = \frac{\pi_{\theta}(y_{i,t}|x, y_{i,<t})}{\pi_{\theta_{\text{old}}}(y_{i,t}|x, y_{i,<t})}, \quad \hat{A}_{i,t} = \hat{A}_i = \frac{r(x, y_i) - \text{mean}(\{r(x, y_i)\}_{i=1}^G)}{\text{std}(\{r(x, y_i)\}_{i=1}^G)}, \quad (2)$$

respectively, where all the tokens in y_i share the same advantage as \hat{A}_i .

A concise overview of PPO and GRPO is provided in Appendix A.1. Across all experiments, we adopt DAPO for fair comparison. In principle, any RLVR method can be applied to our TFPI stage.

3 METHODOLOGY

3.1 THINKING-FREE MODE ENABLES MORE EFFICIENT REASONING

To generate a response $y \sim \pi_{\theta}(\cdot | x)$ for a query x using an SFT-distilled LRM π_{θ} , the query is typically formatted with a chat template. Template 1 illustrates the template adopted by the Qwen model family (Yang et al., 2025a). We define *ThinkingFree* as an operator that transforms an input query x into a modified query $x' = \text{ThinkingFree}(x)$, in which the thinking content is explicitly omitted. Under this transformation, response generation follows $y \sim \pi_{\theta}(\cdot | x')$. This mechanism provides explicit control over whether reasoning content is present or absent in the generated output (see Template 2). Additional examples using other chat templates are provided in Appendix A.2. Hereinafter, we use x to denote a query formatted with the thinking template (e.g., Template 1), and x' or *ThinkingFree*(x) to denote the corresponding thinking-free version (e.g., Template 2).

Template 1 (Thinking Mode) <|im_start|>system\nPlease reason step by step, and put your final answer within \\boxed{.}<|im_end|>\n<|im_start|>user\n{question (x)}<|im_end|>\n<|im_start|>assistant\n

Template 2 (Thinking-Free Mode) <|im_start|>system\nPlease reason step by step, and put your final answer within \\boxed{.}<|im_end|>\n<|im_start|>user\n{question (x)}<|im_end|>\n<|im_start|>assistant\n<think>\n</think>

During inference, converting x into its thinking-free version x' can substantially reduce token consumption. To assess how this transformation affects the reasoning capability of SFT-distilled LRMs, we evaluate DeepSeek-Distilled-Qwen-1.5B (abbreviated as DS-1.5B) and Qwen3-4B on the AIME25. Detailed experimental setup is delayed to Appendix B.1. As shown in Figure 2 (Left), applying the *ThinkingFree* reduces the number of output tokens by more than 70% for both models. It is worth noting that Qwen3-4B is a fast-slow fusion model, whereas DS-1.5B is an SFT-distilled long-CoT model; nevertheless, both exhibit the same trend.

3.2 THINKING-FREE TRAINING IS BENEFICIAL TO SLOW-THINKING

To train an SFT-distilled LRM, the training response length should not be too short (Setlur et al., 2025), as this is detrimental to testing performance (An et al., 2025). As evidenced by the dotted

line in Figure 2 (Right), training Qwen-3-4B with a 4K response length using DAPO indeed leads to a substantial drop in performance on AIME25. Given that using the *ThinkingFree* variant for inference can significantly reduce token consumption, we pose an audacious question: can we apply the *ThinkingFree* operation to all input queries during the rollout stage of RLVR? Moreover, will this approach be beneficial to preserving the original slow-thinking capability of the trained LLM?

Surprisingly, **RL trained with *ThinkingFree* rollout can slightly improve accuracy and reduce token consumption when evaluated in thinking mode, even with very short training context lengths.** Figure 2 (Right) illustrates the training dynamics of Qwen-3-4B trained with a 4K response length under the *ThinkingFree* transformation of queries (detailed settings are in Appendix B.2). Even with a 4K output length, *ThinkingFree* RL increases the accuracy on AIME25 in thinking mode by approximately 2%, while reducing output tokens by around 20%. In contrast, standard RLVR with a 4K length reduces avg@32 by more than 40%. These results suggest that applying *ThinkingFree* during rollout can yield steady improvements with minimal training compute.

3.3 THINKING FREE POLICY INITIALIZATION

Hu et al. (2025) introduce a pre-pretraining stage using formal language to accelerate convergence of pretraining, while Wang et al. (2025b) propose a mid-training stage between pretraining and RL-zero to facilitate RLVR. Inspired by these works, we ask: *can a dedicated stage for SFT-distilled LRM improve the efficiency and effectiveness of standard RLVR scaling? ThinkingFree* RL, which enhances slow-thinking within short training context windows, requires substantially less compute than standard RLVR. Initializing RLVR with a *ThinkingFree* RL policy could therefore reduce rollout tokens while achieving stronger downstream performance. We term this step as **Thinking Free Policy Initialization (TFPI)**, a stage preceding standard RLVR for SFT-distilled LRM that aims to lower rollout costs, raise the ceiling of reasoning ability, and accelerate convergence.

Consider the RLVR objective $\mathcal{J}_{\text{RLVR}}(\theta) = \mathbb{E}_{x \sim \mathcal{D}} [\mathcal{J}_{\text{RLVR}}(\theta, x)]$, where $\mathcal{J}_{\text{RLVR}}(\theta, x)$ denotes the per-example objective of any RLVR algorithm (e.g., DAPO in eq. (1) or GRPO in eq. (5)). For the TFPI stage, we use a modified objective: $\mathcal{J}_{\text{TFPI}}(\theta) = \mathbb{E}_{x \sim \mathcal{D}} [\mathcal{J}_{\text{RLVR}}(\theta, \mathbf{x}')]$, where $\mathbf{x}' = \text{ThinkingFree}(\mathbf{x})$. In the rollout stage of TFPI, G responses are generated conditioned on \mathbf{x}' : $\{y_i\}_{i=1}^G \sim \pi_{\theta_{\text{old}}}(\cdot | \mathbf{x}')$. The importance ratios and advantages (eq. (2)) are then adapted as:

$$r_{i,t}(\theta) = \frac{\pi_{\theta}(y_{i,t} | \mathbf{x}', y_{i,< t})}{\pi_{\theta_{\text{old}}}(y_{i,t} | \mathbf{x}', y_{i,< t})}, \quad \hat{A}_{i,t} = \hat{A}_i = \frac{r(\mathbf{x}', y_i) - \text{mean}(\{r(\mathbf{x}', y_j)\}_{j=1}^G)}{\text{std}(\{r(\mathbf{x}', y_j)\}_{j=1}^G)}, \quad (3)$$

where [Template 1](#) and [Template 2](#) showcase the correspondence between \mathbf{x} and \mathbf{x}' and $r(\mathbf{x}', y) = r(\mathbf{x}, y)$ since the *ThinkingFree* operator does not alter the ground-truth answer of the original problem. In our experiments, we instantiate RLVR with DAPO, i.e., $\mathcal{J}_{\text{RLVR}}(\theta) = \mathcal{J}_{\text{DAPO}}(\theta)$ (see eq. (1)). [Note that Heuristics for RLVR](#) (e.g., multi-stage RL, data curricula) can be directly applied to TFPI.

4 EXPERIMENTS

4.1 EXPERIMENTAL SETTINGS

In this section, we provide a brief overview of the key experimental setup, including training procedures, baselines, and evaluation details. Additional information can be found in Appendix C.

Training Details. We build on the VeRL codebase (Sheng et al., 2024) with RLVR, following the DAPO recipe (Yu et al., 2025), which enables dynamic sampling and clipping higher. All methods use the same hyperparameters (batch size 256, learning rate 1×10^{-6} , no warm-up) and rollout settings (temperature 1, topp 1, topk -1, 8 rollouts/problem). Training is conducted on DS-1.5B, Qwen3-4B, and DS-7B using Polaris-53K (An et al., 2025). Direct RLVR uses a maximum output length of 16K for DS-1.5B/DS-7B and 32K for Qwen3-4B, while TFPI adopts multi-stage training: 2K \rightarrow 4K \rightarrow 8K for DS-1.5B/DS-7B and 4K \rightarrow 8K \rightarrow 16K for Qwen3-4B.

Baselines. We compare TFPI with direct RLVR training from an SFT-distilled LRM (“Direct RL”) under matched total training compute (Table 1). To assess TFPI as a pre-RLVR stage, we run “TFPI + RL” with similar compute and compare against “Direct RL” (Table 2), also including competitive LRM of the same size, such as Polaris (An et al., 2025), DeepScaleR (Luo et al., 2025b), Skywork-OR1 (He et al., 2025), and so on. For efficiency analysis, we compare with several RL-based

216 Table 1: Results of TFPI vs. direct RL across different benchmarks. “Avg@k” denotes the average
 217 accuracy (%) over k random generations (i.e., pass@1). All models are evaluated in thinking mode.
 218 The total training compute for the 3 stages of TFPI equals that of “Direct RL” for fair comparison.
 219 Darker colors in the cell background denote better results within each model group.

Models	Mathematics			Multi-Task	Code	Instruction	Overall
	AIME 24 Avg@32	AIME 25 Avg@32	Beyond AIME Avg@8	GPQA Avg@8	LiveCode Avg@8	IFEval Avg@4	Overall Avg.
DeepSeek-Distill-Qwen-1.5B							
Initial Model	29.6	23.0	8.7	16.3	17.7	36.6	22.0
- Direct RL	33.9	27.1	11.9	19.2	18.2	41.8	25.3
- TFPI stage 1	32.1	26.9	13.9	29.3	18.4	39.5	26.7
- TFPI stage 2	36.8	28.4	14.5	27.8	20.5	42.3	28.4
- TFPI stage 3	40.1	30.8	13.8	29.6	19.9	40.8	29.2
Qwen3-4B							
Initial Model	73.6	68.3	43.4	56.8	54.9	64.9	60.3
Direct RL	75.7	67.0	43.6	56.3	52.5	66.0	60.2
TFPI stage 1	75.2	67.8	42.4	57.9	55.3	66.0	60.8
TFPI stage 2	76.0	68.2	44.7	57.8	54.8	64.8	61.0
TFPI stage 3	79.9	70.6	46.7	58.5	57.0	70.2	63.8
DeepSeek-Distill-Qwen-7B							
Initial Model	56.3	40.0	25.0	36.9	39.5	55.3	42.2
- Direct RL	57.9	40.4	26.6	38.0	38.3	56.7	43.0
- TFPI stage 1	59.4	40.4	29.2	49.0	39.6	56.2	45.6
- TFPI stage 2	61.8	43.9	31.5	48.0	42.0	57.1	47.4
- TFPI stage 3	62.0	44.6	31.1	46.8	42.1	60.2	47.8

241 efficient reasoning baselines (Table 3) under the same evaluation for fair comparison, including
 242 TLMRE (Arora & Zanette, 2025), AdaptThink (Zhang et al., 2025b), AutoThink (Tu et al., 2025),
 243 Laser (Liu et al., 2025a), L1Max (Aggarwal & Welleck, 2025), and ThinkLess (Fang et al., 2025).
 244

245 **Evaluation Details.** Our evaluation benchmarks cover: ❶ **Math Reasoning:** AIME24/25 and Be-
 246 yondAIME (ByteDance-Seed, 2025). ❷ **Multi-Task Reasoning:** GPQA-Diamond (Rein et al.,
 247 2024). ❸ **Code Generation:** LiveCodeBench (Jain et al., 2024). ❹ **Instruction Following:** IFE-
 248 eval (Zhou et al., 2023). Following Guo et al. (2025), we generate multiple outputs (ranging from
 249 4 to 32 depending on the size of the test set) per problem and report pass@1 accuracy. Note that
 250 ❶ is in-domain evaluation, and ❷ ❸ ❹ are out-of-domain evaluation. For IFEval, we report the
 251 *strict prompt* accuracy. All evaluation scripts are adapted from the DeepscaleR codebase (Luo et al.,
 252 2025b). Following the officially recommended decoding parameters¹, we set the temperature to 0.6
 253 and top-p to 0.95 for the thinking mode, and 0.7, 0.8 for the thinking-free mode, respectively. The
 254 maximum output length is 32k for all configurations, except for the Qwen3-4B thinking mode,
 255 where 48k is used to reduce the clipping ratio. Further details are provided in Appendix C.3, and
 256 the effects of changing decoding parameters are presented in Appendix F.4.

257 4.2 TFPI ENHANCES THE SLOW-THINKING OF DISTILLED REASONING MODELS

258 To evaluate the impact of TFPI on the slow-thinking capabilities, we present the results of TFPI
 259 versus “Direct RL” under the same training compute in Table 1. From the table, we have:

260 ❶ **TFPI substantially enhances the slow-thinking capabilities of distilled LRM**s even when
 261 **trained with a small response length.** For example, on DS-1.5B, TFPI Stage 1 raises the overall
 262 average accuracy from 22.0% to 26.7% (+4.7%) despite being restricted to a 2K training response
 263 length. Results of DS-1.5B continue to improve through stages 1 to 3 on AIME25, accuracy
 264 increases from 23.0% (initial model) to 26.9% after Stage 1, 28.4% after Stage 2, and 30.8% after
 265 Stage 3, representing a total gain of +7.8%. Similar improvements are observed for Qwen3-4B and
 266 DS-7B. These findings indicate that TFPI enables effective training under low-cost settings (short
 267 context windows), and that combining this with multi-stage RL yields substantial accuracy gains.
 268

269 ¹See Qwen3-4B Hugging Face page and DS-1.5B Hugging Face page.

270 Table 2: Results (%) of RL after TFPI (“TFPI+RL”) vs. “Direct RL” across different benchmarks.
 271 “Avg@ k ” denotes the average accuracy (%) over k random generations (i.e., pass@1). For LRM
 272 models marked with “**”, results are taken from the corresponding reports (see Appendix C.4); results of 4B
 273 models are from our own runs with 48K response length. All models are evaluated in thinking mode.
 274 The total training compute for “TFPI+RL” is matched to that of “Direct RL” for fair comparison.
 275 Darker colors in the cell background denote better results.

Models	Mathematics			Multi-Task	Code	Instruction	Overall
	AIME 24 Avg@32	AIME 25 Avg@32	Beyond AIME Avg@8	GPQA Avg@8	LiveCode Avg@8	IFEval Avg@4	Overall Avg.
DeepSeek R1*	79.8	65.0	42.4	71.5	64.3	86.1	68.2
Seed-1.5-Thinking*	86.7	74.0	48.0	77.3	64.9	87.4	73.0
Claude4 Opus Thinking*	-	75.5	-	79.6	48.9	89.7	-
Qwen3-235B-Thinking*	85.7	81.5	-	71.1	55.7	83.4	-
Qwen3-4B Direct RL	78.8	71.5	46.4	56.2	54.3	65.1	62.0
Qwen3-4B TFPI stage 3	79.9	70.6	46.7	58.5	57.0	70.2	63.8
Qwen3-4B TFPI + RL	80.8	76.0	49.5	61.1	55.7	71.3	65.7
Qwen3-4B-2507-Thinking - TFPI only	84.7	79.2	51.5	66.4	62.4	68.0	68.7
	89.0	81.2	51.3	70.1	65.5	66.7	70.6

287
 288 **② Compared with “Direct RL”, TFPI delivers faster and larger accuracy improvements under**
 289 **the same training cost.** TFPI outperforms “Direct RL” in nearly all configurations. For example,
 290 Qwen3-4B with TFPI attains 63.8% overall accuracy versus 60.2% for “Direct RL” (+3.6%), while
 291 DS-7B improves by +4.8% (47.8% vs. 43.0%). Given that the equal training compute, these results
 292 imply that TFPI achieves convergence more efficiently than conventional long-CoT RL training.

293 **③ Improvements of TFPI indicate some degree of transfer beyond mathematics.** Although TFPI
 294 is trained solely on Polaris-53K (math-specific data), it demonstrates great out-of-domain improve-
 295 ments as well. For example, on DeepSeek-Distill-Qwen-1.5B, GPQA accuracy increases
 296 from 16.3% to 29.6%, LiveCodeBench from 17.7% to 19.9%, and IFEval from 36.6% to 40.8%
 297 after Stage 3. Notably, **improvements on mathematical benchmarks are often consistent across**
 298 **successive training stages, whereas other domains sometimes exhibit fluctuations** (e.g., GPQA
 299 for DS-7B and LiveCodeBench for DS-1.5B). This suggests that **incorporating more diverse**
 300 **training data spanning multiple domains could be helpful for TFPI.**

301 4.3 TFPI AS A FOUNDATION FOR RLVR TO ACHIEVE HIGHER PERFORMANCE

302 Table 2 shows the representative results between “TFPI + RL” with “Direct RL” under the same
 303 training cost (full results in Table 9 in Appendix F.2). The results lead to the following observations:

304 **① TFPI can raise the upper bound of RL-trained performance.** RL training on a TFPI-trained
 305 model can still yield notable improvements, particularly in mathematics. For example, adding an
 306 RL stage after TFPI for Qwen3-4B boosts AIME25 accuracy from 70.6% to 76.0% (+5.4%).
 307 Similarly, Beyond AIME scores increase by more than 2%. Across different model scales, applying
 308 RL after TFPI consistently achieves higher accuracies than “Direct RL” under the same compute
 309 budget. For instance, on Qwen3-4B, the overall accuracy rises from 62.0% (Direct RL) to 65.7%
 310 (TFPI+RL). These results suggest that incorporating TFPI as an intermediate stage between long
 311 CoT distillation and standard RLVR can be beneficial for elevating final performance.

312 **② TFPI + RL is an effective and efficient strategy for training high-performing LRM.** From
 313 Figure 1 (Left), the total compute cost of all three TFPI stages amounts to less than 20% of stan-
 314 dard RL training with 32K token sequences. From Table 2, for DS-7B, TFPI+RL achieves ap-
 315 proximately the same overall performance as Polaris-7B-Preview, despite using a maximum
 316 response length of 16K, whereas Polaris-7B-Preview follows a 16K → 24K → 32K pro-
 317 gression during RL. Similarly, Polaris-4B-Preview employs a 40K → 48K → 52K length
 318 schedule and consumes approximately 8K H800 GPU hours, while our TFPI+RL requires only
 319 about 1.5K H800 GPU hours (see Appendix C.1) and achieves superior performance under 48K
 320 testing length. Even without a subsequent RL stage, TFPI alone allows DS-1.5B to outperform
 321 DeepScaleR, which uses a maximum training length of 24K. Using only TFPI (4K→8K→16K),
 322 Qwen3-4B-2507 achieves 89% accuracy on AIME24. Remarkably, this 4B model outperforms
 323 Qwen3-235B-Thinking in math reasoning and code generation. These findings suggest that

324
 325 Table 3: Comparison of the Thinking-Free inference mode of TFPI with efficient reasoning baselines
 326 across various reasoning tasks. “Avg@k” denotes the average accuracy (in %) over k generations
 327 (i.e., pass@1), and “Toks” indicates the average output length in thousands of tokens (K). Models
 328 with “*” are trained from DeepScaleR-1.5B, while the remaining are from DS-1.5B. Darker
 329 cell background colors indicate better results.

330 Models	331 AIME 24		332 AIME 25		333 Beyond AIME		334 GPQA		335 Overall	
	336 avg@32	337 Toks	338 avg@32	339 Toks	340 avg@8	341 Toks	342 avg@8	343 Toks	344 Avg.	345 Toks
1) TLMRE-DS-1.5B ($\alpha = 0.1$)	27.6	12.9	24.8	12.5	9.2	11.9	14.8	7.5	19.1	11.2
2) AdaptThink-1.5B ($\delta = 0.05$)	28.1	8.0	22.6	7.9	10.0	4.8	14.8	5.1	18.9	6.5
3) AutoThink-DS-1.5B-Stage3	30.3	10.2	25.2	9.1	9.4	8.7	17.4	7.0	20.6	8.7
4) Laser-DE-L4096-1.5B	30.3	8.3	24.9	7.4	9.7	7.4	21.1	4.7	21.5	6.9
5) AutoThink-Stage3*	38.9	8.7	28.9	7.7	11.6	7.8	27.3	5.4	26.7	7.4
6) L1-1.5B-Max*	27.2	3.2	26.3	2.9	9.1	3.1	32.4	2.3	23.8	2.9
7) Thinkless-1.5B-RL*	28.4	11.3	24.1	11.1	8.1	11.7	20.3	12.7	20.2	11.7
DS-1.5B (Thinking)	29.6	16.7	23.0	16.5	8.7	14.4	16.3	9.8	19.4	14.3
DS-1.5B (Thinking-Free)	12.4	5.7	10.9	4.4	4.4	3.4	4.2	0.9	8.0	3.6
- TFPI stage 1	21.9	1.6	15.3	1.4	8.7	1.3	32.9	0.8	19.7	1.3
- TFPI stage 2	31.5	3.4	24.2	3.1	10.1	2.9	35.3	1.6	25.3	2.7
- TFPI stage 3	37.5	5.3	28.4	5.0	12.4	4.9	35.6	2.6	28.5	4.4

340
 341 TFPI can serve both as a strong standalone training approach and as an efficient foundation for
 342 subsequent RL, producing competitive LRM_s with significantly reduced compute requirements.
 343

344 4.4 TFPI IMPROVES THE TOKEN EFFICIENCY OF DISTILLED REASONING MODELS

345 We compare the thinking-free inference with other RL-based efficient reasoning baselines in 1.5B
 346 size in Table 3 (see also Table 10 in Appendix F.2). We draw the following conclusions:

347 **1 Both accuracy and token efficiency steadily improve after stage 3 of TFPI.** For DS-1.5B,
 348 thinking-free accuracy on AIME24 increases from 29.6% (initial model) to 37.5% (TFPI stage 3),
 349 while the average output length remains substantially shorter than that of the original thinking mode
 350 (5.3K vs. 16.7K tokens). A similar trend is observed for Qwen3-4B, where accuracy improves
 351 from 26.9% to 75.1% across stages, with output lengths still far below those of the original thinking
 352 model. These results demonstrate that TFPI naturally produces more token-efficient LRM_s, offering
 353 an alternative pathway to train models that deliver both high accuracy and reduced output length.
 354

355 **2 Compared with other RL-based token control methods, TFPI achieves the best performance–efficiency trade-off without specialized reward or training designs.** In DS-1.5B, both
 356 TFPI stage 2 and stage 3 outperform almost all baselines in terms of overall accuracy while main-
 357 taining competitive or lower token usage. We visualize the overall accuracy–token usage trade-off
 358 in Figure 1 (Right), where TFPI consistently lies on the Pareto frontier across different stages. This
 359 observation motivates a rethinking of existing “token-efficient reasoning RL designs” that rely heavily
 360 on specialized length reward shaping: training with TFPI offers an alternative paradigm in which
 361 a strong slow-thinking LRM can be obtained, and a more efficient variant can be realized simply by
 362 switching to the thinking-free mode without any additional length-control mechanisms.
 363

364 5 ANALYSIS

365 5.1 WHY TFPI LEADS TO BETTER THINKING-MODE INFERENCE?

366 In this section, we delve deeper into why TFPI, which leverages void thinking content in Template 2,
 367 can generalize to enhance reasoning in Template 1. We analyze DS-1.5B from two perspectives:

368 **1 Behavioural level:** The learned *verification* behaviours after `</think>` during TFPI can gen-
 369 eralize to the slow-thinking verification occurring within the `<think>` and `</think>`. The blue
 370 lines in Figure 3 show the ratio of verification steps (i.e., the number of verification steps divided by
 371 the total number of steps; see Appendix D for details) for the training set (thinking-free mode) and
 372 AIME 25 dataset (thinking mode). We observe that the verification ratio exhibits a similar trend:
 373 a rapid drop in Stage 1, followed by steady growth in Stage 2, and a sharp increase in Stage 3.
 374 Notably, the sharp decline in Stage 1 resembles an information compression process. In Stages 2
 375 and 3, the model begins to explore more extensively (Figure 3 Right), which may explain why
 376

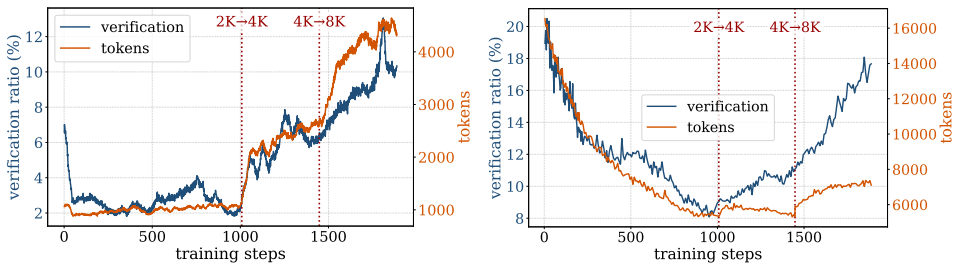


Figure 3: Behaviour-Level Analysis of DS-1.5B over the TFPI Training Course. The ratio of verification steps and the average output tokens over training steps on the training set in thinking-free mode (**Left**) and on AIME25 in thinking mode (**Right**) in 3 stages of TFPI.

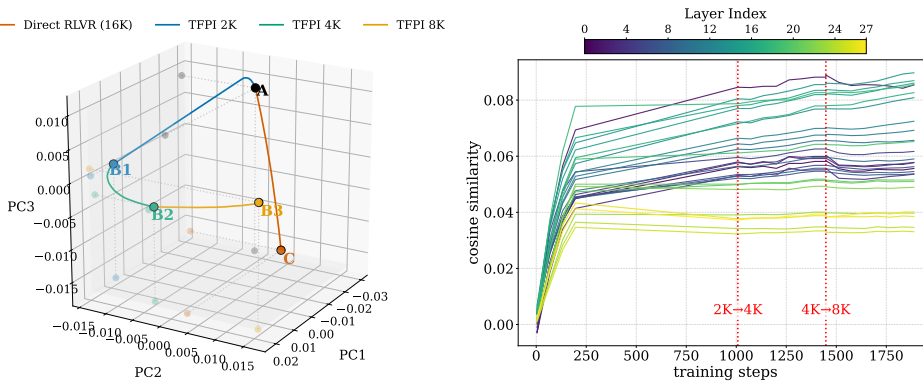


Figure 4: Parameter-Level Analysis. **Left:** PCA projection of model parameters from DS-1.5B to final checkpoints. TFPI (blue) starts at **A**, passes through intermediate points (**B1**, **B2**, **B3**), and ultimately converges near the Direct RL final checkpoint (**C**). **Right:** Cosine similarity between parameter updates of TFPI-trained checkpoints and (C-A) across layers during training.

TFPI achieves superior performance. As verification is believed to be vital for slow-thinking reasoning (Setlur et al., 2025), the observed generalization of verification behavior suggests a transfer from thinking-free training to inference in thinking mode.

2 Parameter level: TFPI explores the parameter space more extensively at a faster pace, with its parameter update directions progressively aligning with those of “Direct RL.” As shown in Figure 4 (Left), the PCA visualization of the initial model, TFPI-trained checkpoints, and Direct RL checkpoints exhibits distinct trajectories in parameter space. The TFPI begins from the initial model (**A**), moves through intermediate points (**B1**, **B2**, and **B3**), and ultimately converges to a region near the Direct RL final checkpoint (**C**). This indicates that TFPI traverses a larger and more diverse region of parameter space before reaching a point close to the RL-trained model. Such broad exploration may help explain why TFPI can lead to better LRMAs. Furthermore, Figure 4 (Right) shows that the cosine similarity of parameter updates between the TFPI-trained checkpoints and the Direct RL final checkpoint steadily increases across nearly all layers throughout training. This suggests that during TFPI training, the parameter updates share similarities with those in standard long-CoT training. [To make our analysis more robust, additional results are given in Appendix F.1.](#)

5.2 ABOUT REASONING PATTERN AND ROLLOUT SPEED

TFPI Preserves the Reasoning Pattern of Thinking Mode. In *thinking mode* (Template 1), a response y comprises a long *thinking* section and a concise *answer* y^{ans} . In *ThinkingFree* mode (Template 2), the thinking section is omitted, and y^{ans} contains a shorter reasoning path. While standard RL tends to lengthen the thinking part, TFPI increases the length of y^{ans} due to the absence of explicit thinking. As shown in Figure 5 (Left), for DS-1.5B trained with TFPI and evaluated in thinking mode, $|y^{\text{ans}}|$ remains stable at 500–580 tokens, whereas $|y^{\text{ans}}|/|y|$ rises as the total length $|y|$ decreases. This indicates that TFPI preserves the core reasoning pattern of slow-thinking rather than drifting toward an excessively extended “slow-slow thinking” behavior.

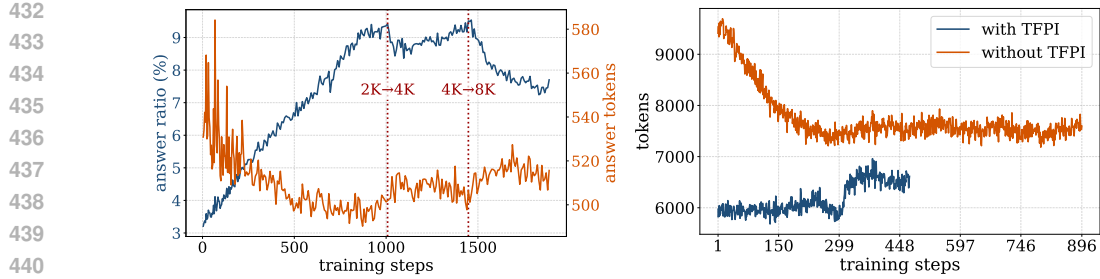


Figure 5: **Left:** For TFPI with DS-1.5B on AIME25 in thinking mode, showing the average number of answer tokens (excluding the thinking part) and the ratio of answer length to total response length over training steps. **Right:** For long CoT RL with DS-1.5B, showing the average number of tokens during rollout on the training set over training steps, with and without the TFPI stage.

Table 4: Additional results of TFPI. All models are evaluated in thinking mode.

Models	AIME 24	AIME 25	Beyond AIME	GPQA	LiveCode	IFEval	Overall
Stage Schedule Sensitivity, Qwen3-4B							
4K → 8K → 16K	79.9	70.6	46.7	58.5	57.0	70.2	63.8
8K → 16K	78.0	70.2	46.7	59.5	55.8	64.5	62.4
16K only	77.1	71.5	45.8	56.4	54.4	66.0	61.9
Multi-Stage Direct RL, Qwen3-4B							
TFPI Stage 3	79.9	70.6	46.7	58.5	57.0	70.2	63.8
Multi-Stage Direct RL	64.9	48.6	32.5	55.2	51.0	65.2	52.9
Qwen3-14B							
Initial Model	81.7	73.2	50.2	65.0	63.5	67.3	66.8
- Direct RL	81.7	74.5	50.8	64.8	61.8	68.2	66.9
- TFPI stage 3	83.2	76.0	50.5	65.6	63.8	67.8	67.8
Qwen3-14B Tokens (K)							
Initial Model	16.8	20.8	22.8	9.4	16.0	-	17.1
- Direct RL	17.9	22.1	24.5	10.4	17.4	-	18.5
- TFPI stage 3	13.8	17.3	18.3	7.3	13.8	-	14.1

TFPI Speeds Up Rollout for Long-CoT RL Training. Another advantage of TFPI is its ability to speed up the rollout stage in standard long-CoT RL training. As shown in Figure 5 (Right), when directly performing RL from DS-1.5B, the average output tokens during rollout on the training set start at over 9K, decrease to around 7.5K within the first 300 steps, and then fluctuate around 7.5K in the later stages. In contrast, when RL is performed after the TFPI phase, the average output tokens start at only 6K and the maximum length is below 7K tokens.

5.3 SCALING UP MODEL SIZE

To assess the effect of TFPI on larger reasoning models, we conducted experiments with Qwen3-14B under the same settings as Qwen3-4B. As shown in Table 4, TFPI still outperforms Direct RL under the same training compute. Notably, Direct RL yields results only comparable to those of the initial model (66.9% vs. 66.8% on average). We hypothesize that Polaris-53K is, in some sense, too easy for Qwen3-14B (with over 78% rollout accuracy), leaving only approximately 30% effective data after dynamic sampling (excluding 0/8 and 8/8 prompts). Nonetheless, TFPI remains effective in this setting. Additionally, TFPI reduces the average number of output tokens on the test set by 23.8% even in thinking mode (14.1K vs. 18.5K). These results highlight the effectiveness of TFPI for larger model sizes, and we believe that with more challenging, higher-quality data, TFPI can further realize its scalability potential.

5.4 ABLATION STUDY

Stage Schedule Sensitivity. To assess sensitivity to the stage schedule, we train Qwen3-4B under alternative schedules (8K → 16K and 16K-only) with approximately matched compute budgets. As

486 shown in Table 4, all schedules outperform the Direct RL baseline and achieve comparable performance
 487 on math benchmarks, indicating that TFPI is robust to the choice of schedule. Nevertheless,
 488 $4K \rightarrow 8K \rightarrow 16K$ yields the best overall results (63.8% vs. 62.4% and 61.9%). We hypothesize
 489 that this stems from an implicit data curriculum induced by dynamic sampling: beginning at 4K
 490 improves training efficiency and emphasizes easier problems early on.

491 **Multi-Stage Direct RL.** As discussed in Section 3.2 and Figure 2 (right), applying Direct RL with a
 492 4K response length causes a substantial performance drop on AIME25 for Qwen3-4B. In contrast,
 493 TFPI trains stably even at 4K. This indicates that, even in a multi-stage setting, the initial stage length
 494 should not be too short. To rule out the potential artifact introduced by multi-stage training, we run
 495 Direct RL with the identical multi-stage schedule on Qwen3-4B. As shown in Table 4, Direct RL
 496 still incurs a substantial performance decrease under the $4K \rightarrow 8K \rightarrow 16K$ schedule. Additional
 497 details are provided in Appendix F.7.

500 6 RELATED WORK

501 **503 LRM & Efficiency RLVR.** RLVR has enabled the development of numerous high-performing
 504 large reasoning models (LRMs) (Yang et al., 2025a; Zeng et al., 2025a; An et al., 2025), inspiring
 505 research on model behaviors (Liu et al., 2025b; Wang et al., 2025a), novel algorithms (Liu et al.,
 506 2025b; Zheng et al., 2025), multimodal extensions (Meng et al., 2025; Xiao et al., 2025; Wang et al.,
 507 2025c), tool integration (Jin et al., 2025; Feng et al., 2025; Li et al., 2025a; Xue et al., 2025; Team
 508 et al., 2025a), and other related directions (Xu et al., 2025a; Zhang et al., 2025a; Chen et al., 2025c;
 509 Zhang et al., 2025c). RLVR can be applied directly to base LLMs (“RL zero”) (Zeng et al., 2025b;
 510 Guo et al., 2025) or initialized from SFT-distilled long-CoT models, the latter typically yielding
 511 stronger results (Luo et al., 2025b; An et al., 2025). A major challenge for RLVR is the cost of
 512 training with long contexts, as longer outputs are often necessary for harder tasks (Shrivastava et al.,
 513 2025; Zeng et al., 2025a), consuming high computational resources. Multi-stage RLVR mitigates
 514 this by starting with shorter contexts and gradually extending them (Luo et al., 2025b; An et al.,
 515 2025; He et al., 2025), while algorithmic approaches modify GRPO to reduce length bias (Yu et al.,
 516 2025; Liu et al., 2025b; Wang et al., 2025a). Orthogonal to these strategies, we introduce TFPI as a
 517 lightweight stage before RLVR, improving efficiency and strengthening the slow-thinking mode at
 518 inference with minimal training cost, thus facilitating more effective subsequent RLVR.

519 **Efficient Reasoning.** To address the issue of overthinking (Chen et al., 2024; Sui et al., 2025), con-
 520 siderable efforts have been made, including prompt-based methods (Muennighoff et al., 2025; Yang
 521 et al., 2025c; Fu et al., 2025a; Chen et al., 2025a; Fu et al., 2025b), SFT-based approaches (Kang
 522 et al., 2025; Ma et al., 2025; Munkhbat et al., 2025; Luo et al., 2025a), and RL-related designs. RL-
 523 related approaches can be further categorized into length-based reward shaping (Team et al., 2025b;
 524 Aggarwal & Welleck, 2025; Arora & Zanette, 2025; Liu et al., 2025a), integration of fast and slow
 525 thinking (Fang et al., 2025; Zhang et al., 2025b; Lou et al., 2025; Tu et al., 2025; Jiang et al., 2025;
 526 Zhang et al., 2025d), and thinking budget control (Li et al., 2025b; Hammoud et al., 2025; Wen
 527 et al., 2025). These methods primarily trade accuracy for efficiency and rely on specialized reward
 528 functions or training strategies to encourage more efficient reasoning. In contrast, our proposed
 529 TFPI naturally yields even more efficient LRM without specialized rewards or training designs.

531 7 CONCLUSION

532 After recognizing the benefits of *ThinkingFree* for both inference and the training of distilled reason-
 533 ing models, we introduce TFPI, a cost-efficient intermediate stage between long-CoT distillation and
 534 standard RL training. As a strong initialization point, TFPI accelerates RL convergence, enhances
 535 attainable performance, and promotes more token-efficient reasoning without complex reward shap-
 536 ing or elaborate training pipelines. We further explain the factors behind TFPI’s success from both
 537 the behavioral and parameter levels. Overall, TFPI provides a complementary path for building
 538 “token-efficient” LRM, offering an effective and efficient alternative to current RL paradigms.

540 REFERENCES
541

542 Pranjal Aggarwal and Sean Welleck. L1: Controlling how long a reasoning model thinks with
543 reinforcement learning. *arXiv preprint arXiv:2503.04697*, 2025.

544 Chenxin An, Zhihui Xie, Xiaonan Li, Lei Li, Jun Zhang, Shansan Gong, Ming Zhong, Jingjing
545 Xu, Xipeng Qiu, Mingxuan Wang, and Lingpeng Kong. Polaris: A post-training recipe for scal-
546 ing reinforcement learning on advanced reasoning models, 2025. URL <https://hkunlp.github.io/blog/2025/Polaris>.

547

548 Daman Arora and Andrea Zanette. Training language models to reason efficiently. *arXiv preprint*
549 *arXiv:2502.04463*, 2025.

550

551 ByteDance-Seed. Beyondaime: Advancing math reasoning evaluation beyond high
552 school olympiads. <https://huggingface.co/datasets/ByteDance-Seed/BeyondAIME>, 2025. Hugging Face repository.

553

554 Runjin Chen, Zhenyu Zhang, Junyuan Hong, Souvik Kundu, and Zhangyang Wang. Seal: Steerable
555 reasoning calibration of large language models for free. *arXiv preprint arXiv:2504.07986*, 2025a.

556

557 Tianhao Chen, Xin Xu, Zijing Liu, Pengxiang Li, Xinyuan Song, Ajay Kumar Jaiswal, Fan Zhang,
558 Jishan Hu, Yang Wang, Hao Chen, et al. Gpas: Accelerating convergence of llm pretraining via
559 gradient-preserving activation scaling. *arXiv preprint arXiv:2506.22049*, 2025b.

560

561 Xingyu Chen, Jiahao Xu, Tian Liang, Zhiwei He, Jianhui Pang, Dian Yu, Linfeng Song, Qizhi Liu,
562 Mengfei Zhou, Zhuosheng Zhang, et al. Do not think that much for 2+ 3=? on the overthinking
563 of o1-like llms. *arXiv preprint arXiv:2412.21187*, 2024.

564

565 Zigeng Chen, Xinyin Ma, Gongfan Fang, Ruonan Yu, and Xinchao Wang. Verithinker: Learning to
566 verify makes reasoning model efficient. *arXiv preprint arXiv:2505.17941*, 2025c.

567

568 Gongfan Fang, Xinyin Ma, and Xinchao Wang. Thinkless: Llm learns when to think. *arXiv preprint*
569 *arXiv:2505.13379*, 2025.

570

571 Jiazhan Feng, Shijue Huang, Xingwei Qu, Ge Zhang, Yujia Qin, Baoquan Zhong, Chengquan Jiang,
572 Jinjin Chi, and Wanjun Zhong. Retool: Reinforcement learning for strategic tool use in llms.
573 *arXiv preprint arXiv:2504.11536*, 2025.

574

575 Yichao Fu, Junda Chen, Yonghao Zhuang, Zheyu Fu, Ion Stoica, and Hao Zhang. Reasoning without
576 self-doubt: More efficient chain-of-thought through certainty probing. In *ICLR 2025 Workshop*
577 *on Foundation Models in the Wild*, 2025a.

578

579 Yichao Fu, Xuewei Wang, Yuandong Tian, and Jiawei Zhao. Deep think with confidence. *arXiv*
580 *preprint arXiv:2508.15260*, 2025b.

581

582 Daya Guo, Dejian Yang, Haowei Zhang, Junxiao Song, Ruoyu Zhang, Runxin Xu, Qihao Zhu,
583 Shirong Ma, Peiyi Wang, Xiao Bi, et al. Deepseek-r1: Incentivizing reasoning capability in llms
584 via reinforcement learning. *arXiv preprint arXiv:2501.12948*, 2025.

585

586 Hasan Abed Al Kader Hammoud, Kumail Alhamoud, Abed Hammoud, Elie Bou-Zeid, Marzyeh
587 Ghassemi, and Bernard Ghanem. Train long, think short: Curriculum learning for efficient rea-
588 soning. *arXiv preprint arXiv:2508.08940*, 2025.

589

590 Jujie He, Jiacai Liu, Chris Yuhao Liu, Rui Yan, Chaojie Wang, Peng Cheng, Xiaoyu Zhang, Fuxiang
591 Zhang, Jiacheng Xu, Wei Shen, et al. Skywork open reasoner 1 technical report. *arXiv preprint*
592 *arXiv:2505.22312*, 2025.

593

594 Michael Y Hu, Jackson Petty, Chuan Shi, William Merrill, and Tal Linzen. Between circuits
595 and chomsky: Pre-pretraining on formal languages imparts linguistic biases. *arXiv preprint*
596 *arXiv:2502.19249*, 2025.

597

598 Zhen Huang, Zengzhi Wang, Shijie Xia, Xuefeng Li, Haoyang Zou, Ruijie Xu, Run-Ze Fan, Lyu-
599 manshan Ye, Ethan Chern, Yixin Ye, et al. Olympicarena: Benchmarking multi-discipline cog-
600 nitive reasoning for superintelligent ai. *Advances in Neural Information Processing Systems*, 37:
601 19209–19253, 2024.

594 Aaron Jaech, Adam Kalai, Adam Lerer, Adam Richardson, Ahmed El-Kishky, Aiden Low, Alec
 595 Helyar, Aleksander Madry, Alex Beutel, Alex Carney, et al. Openai o1 system card. *arXiv*
 596 *preprint arXiv:2412.16720*, 2024.

597

598 Naman Jain, King Han, Alex Gu, Wen-Ding Li, Fanjia Yan, Tianjun Zhang, Sida Wang, Armando
 599 Solar-Lezama, Koushik Sen, and Ion Stoica. Livecodebench: Holistic and contamination free
 600 evaluation of large language models for code. *arXiv preprint arXiv:2403.07974*, 2024.

601

602 Lingjie Jiang, Xun Wu, Shaohan Huang, Qingxiu Dong, Zewen Chi, Li Dong, Xingxing Zhang,
 603 Tengchao Lv, Lei Cui, and Furu Wei. Think only when you need with large hybrid-reasoning
 604 models. *arXiv preprint arXiv:2505.14631*, 2025.

605

606 Bowen Jin, Hansi Zeng, Zhenrui Yue, Jinsung Yoon, Sercan Arik, Dong Wang, Hamed Zamani, and
 607 Jiawei Han. Search-r1: Training llms to reason and leverage search engines with reinforcement
 608 learning. *arXiv preprint arXiv:2503.09516*, 2025.

609

610 Yu Kang, Xianghui Sun, Liangyu Chen, and Wei Zou. C3ot: Generating shorter chain-of-thought
 611 without compromising effectiveness. In *Proceedings of the AAAI Conference on Artificial Intelligence*, volume 39, pp. 24312–24320, 2025.

612

613 Woosuk Kwon, Zhuohan Li, Siyuan Zhuang, Ying Sheng, Lianmin Zheng, Cody Hao Yu, Joseph E.
 614 Gonzalez, Hao Zhang, and Ion Stoica. Efficient memory management for large language model
 615 serving with pagedattention. In *Proceedings of the ACM SIGOPS 29th Symposium on Operating
 Systems Principles*, 2023.

616

617 Xuefeng Li, Haoyang Zou, and Pengfei Liu. Torl: Scaling tool-integrated rl. *arXiv preprint*
 618 *arXiv:2503.23383*, 2025a.

619

620 Zheng Li, Qingxiu Dong, Jingyuan Ma, Di Zhang, and Zhifang Sui. Selfbudgeter: Adaptive token
 621 allocation for efficient llm reasoning. *arXiv preprint arXiv:2505.11274*, 2025b.

622

623 Wei Liu, Ruochen Zhou, Yiyun Deng, Yuzhen Huang, Junteng Liu, Yuntian Deng, Yizhe Zhang,
 624 and Junxian He. Learn to reason efficiently with adaptive length-based reward shaping. *arXiv*
preprint arXiv:2505.15612, 2025a.

625

626 Zichen Liu, Changyu Chen, Wenjun Li, Penghui Qi, Tianyu Pang, Chao Du, Wee Sun Lee,
 627 and Min Lin. Understanding r1-zero-like training: A critical perspective. *arXiv preprint*
arXiv:2503.20783, 2025b.

628

629 Chenwei Lou, Zewei Sun, Xinnian Liang, Meng Qu, Wei Shen, Wenqi Wang, Yuntao Li, Qing-
 630 ping Yang, and Shuangzhi Wu. Adacot: Pareto-optimal adaptive chain-of-thought triggering via
 631 reinforcement learning. *arXiv preprint arXiv:2505.11896*, 2025.

632

633 Haotian Luo, Li Shen, Haiying He, Yibo Wang, Shiwei Liu, Wei Li, Naiqiang Tan, Xiaochun Cao,
 634 and Dacheng Tao. O1-pruner: Length-harmonizing fine-tuning for o1-like reasoning pruning.
 635 *arXiv preprint arXiv:2501.12570*, 2025a.

636

637 Michael Luo, Sijun Tan, Justin Wong, Xiaoxiang Shi, William Y. Tang, Manan Roongta, Colin Cai,
 638 Jeffrey Luo, Li Erran Li, Raluca Ada Popa, and Ion Stoica. Deepscaler: Surpassing o1-preview
 639 with a 1.5b model by scaling rl, 2025b. Notion Blog.

640

641 Xinyin Ma, Guangnian Wan, Rupeng Yu, Gongfan Fang, and Xinchao Wang. Cot-valve: Length-
 642 compressible chain-of-thought tuning. *arXiv preprint arXiv:2502.09601*, 2025.

643

644 Fanqing Meng, Lingxiao Du, Zongkai Liu, Zhixiang Zhou, Quanfeng Lu, Daocheng Fu, Tiancheng
 645 Han, Botian Shi, Wenhui Wang, Junjun He, et al. Mm-eureka: Exploring the frontiers of multi-
 646 modal reasoning with rule-based reinforcement learning. *arXiv preprint arXiv:2503.07365*, 2025.

647

Meredith Ringel Morris, Jascha Sohl-Dickstein, Noah Fiedel, Tris Warkentin, Allan Dafoe, Alek-
 648 sandra Faust, Clement Farabet, and Shane Legg. Levels of agi for operationalizing progress on
 649 the path to agi. *arXiv preprint arXiv:2311.02462*, 2023.

648 Niklas Muennighoff, Zitong Yang, Weijia Shi, Xiang Lisa Li, Li Fei-Fei, Hannaneh Hajishirzi, Luke
 649 Zettlemoyer, Percy Liang, Emmanuel Candès, and Tatsunori Hashimoto. s1: Simple test-time
 650 scaling. *arXiv preprint arXiv:2501.19393*, 2025.

651

652 Tergel Munkhbat, Namgyu Ho, Seo Hyun Kim, Yongjin Yang, Yujin Kim, and Se-Young Yun. Self-
 653 training elicits concise reasoning in large language models. *arXiv preprint arXiv:2502.20122*,
 654 2025.

655 Long Phan, Alice Gatti, Ziwen Han, Nathaniel Li, Josephina Hu, Hugh Zhang, Sean Shi,
 656 Michael Choi, Anish Agrawal, Arnav Chopra, et al. Humanity’s last exam. *ArXiv preprint*,
 657 [abs/2501.14249](https://arxiv.org/abs/2501.14249), 2025. URL <https://arxiv.org/abs/2501.14249>.

658

659 David Rein, Betty Li Hou, Asa Cooper Stickland, Jackson Petty, Richard Yuanzhe Pang, Julien Di-
 660 rani, Julian Michael, and Samuel R Bowman. Gpqa: A graduate-level google-proof q&a bench-
 661 mark. In *First Conference on Language Modeling*, 2024.

662 John Schulman, Filip Wolski, Prafulla Dhariwal, Alec Radford, and Oleg Klimov. Proximal policy
 663 optimization algorithms. *arXiv preprint arXiv:1707.06347*, 2017.

664

665 ByteDance Seed, Jiaze Chen, Tiantian Fan, Xin Liu, Lingjun Liu, Zhiqi Lin, Mingxuan Wang,
 666 Chengyi Wang, Xiangpeng Wei, Wenyuan Xu, et al. Seed1. 5-thinking: Advancing superb rea-
 667 soning models with reinforcement learning. *arXiv preprint arXiv:2504.13914*, 2025.

668

669 Amrith Setlur, Matthew YR Yang, Charlie Snell, Jeremy Greer, Ian Wu, Virginia Smith, Max Sim-
 670 chowitz, and Aviral Kumar. e3: Learning to explore enables extrapolation of test-time compute
 671 for llms. *arXiv preprint arXiv:2506.09026*, 2025.

672

Zihong Shao, Peiyi Wang, Qihao Zhu, Runxin Xu, Junxiao Song, Xiao Bi, Haowei Zhang,
 673 Mingchuan Zhang, YK Li, Yang Wu, et al. Deepseekmath: Pushing the limits of mathemati-
 674 cal reasoning in open language models. *arXiv preprint arXiv:2402.03300*, 2024.

675

Guangming Sheng, Chi Zhang, Zilingfeng Ye, Xibin Wu, Wang Zhang, Ru Zhang, Yanghua Peng,
 676 Haibin Lin, and Chuan Wu. Hybridflow: A flexible and efficient rlhf framework. *arXiv preprint*
 677 *arXiv: 2409.19256*, 2024.

678

Vaishnavi Shrivastava, Ahmed Awadallah, Vidhisha Balachandran, Shivam Garg, Harkirat Behl,
 679 and Dimitris Papailiopoulos. Sample more to think less: Group filtered policy optimization for
 680 concise reasoning. *arXiv preprint arXiv:2508.09726*, 2025.

681

Yang Sui, Yu-Neng Chuang, Guanchu Wang, Jiamu Zhang, Tianyi Zhang, Jiayi Yuan, Hongyi Liu,
 682 Andrew Wen, Shaochen Zhong, Hanjie Chen, et al. Stop overthinking: A survey on efficient
 683 reasoning for large language models. *arXiv preprint arXiv:2503.16419*, 2025.

684

Kimi Team, Yifan Bai, Yiping Bao, Guanduo Chen, Jiahao Chen, Ningxin Chen, Ruijue Chen,
 685 Yanru Chen, Yuankun Chen, Yutian Chen, et al. Kimi k2: Open agentic intelligence. *arXiv*
 686 *preprint arXiv:2507.20534*, 2025a.

687

Kimi Team, Angang Du, Bofei Gao, Bowei Xing, Changjiu Jiang, Cheng Chen, Cheng Li, Chenjun
 688 Xiao, Chenzhuang Du, Chonghua Liao, et al. Kimi k1. 5: Scaling reinforcement learning with
 689 llms. *arXiv preprint arXiv:2501.12599*, 2025b.

690

Yuxuan Tong, Xiwen Zhang, Rui Wang, Ruidong Wu, and Junxian He. Dart-math: Difficulty-aware
 691 rejection tuning for mathematical problem-solving. *ArXiv preprint*, [abs/2407.13690](https://arxiv.org/abs/2407.13690), 2024. URL
 692 <https://arxiv.org/abs/2407.13690>.

693

Songjun Tu, Jiahao Lin, Qichao Zhang, Xiangyu Tian, Linjing Li, Xiangyuan Lan, and Dongbin
 694 Zhao. Learning when to think: Shaping adaptive reasoning in rl-style models via multi-stage rl.
 695 *arXiv preprint arXiv:2505.10832*, 2025.

696

Shenzhi Wang, Le Yu, Chang Gao, Chujie Zheng, Shixuan Liu, Rui Lu, Kai Dang, Xionghui Chen,
 697 Jianxin Yang, Zhenru Zhang, et al. Beyond the 80/20 rule: High-entropy minority tokens drive
 698 effective reinforcement learning for llm reasoning. *arXiv preprint arXiv:2506.01939*, 2025a.

699

700

702 Zengzhi Wang, Fan Zhou, Xuefeng Li, and Pengfei Liu. Octothinker: Mid-training incentivizes
 703 reinforcement learning scaling. *arXiv preprint arXiv:2506.20512*, 2025b.
 704

705 Zhenhailong Wang, Xuehang Guo, Sofia Stoica, Haiyang Xu, Hongru Wang, Hyeonjeong Ha, Xiusi
 706 Chen, Yangyi Chen, Ming Yan, Fei Huang, et al. Perception-aware policy optimization for mul-
 707 timodal reasoning. *arXiv preprint arXiv:2507.06448*, 2025c.

708 Jason Wei, Xuezhi Wang, Dale Schuurmans, Maarten Bosma, Brian Ichter, Fei Xia, Ed H. Chi,
 709 Quoc V. Le, and Denny Zhou. Chain-of-thought prompting elicits reasoning in large language
 710 models. In Sanmi Koyejo, S. Mohamed, A. Agarwal, Danielle Belgrave, K. Cho, and A. Oh
 711 (eds.), *Advances in Neural Information Processing Systems 35: Annual Conference on Neural
 712 Information Processing Systems 2022, NeurIPS 2022, New Orleans, LA, USA, November 28 - De-
 713 cember 9, 2022*, 2022. URL [http://papers.nips.cc/paper_files/paper/2022/
 714 hash/9d5609613524ecf4f15af0f7b31abca4-Abstract-Conference.html](http://papers.nips.cc/paper_files/paper/2022/hash/9d5609613524ecf4f15af0f7b31abca4-Abstract-Conference.html).

715

716 Hao Wen, Xinrui Wu, Yi Sun, Feifei Zhang, Liye Chen, Jie Wang, Yunxin Liu, Ya-Qin Zhang,
 717 and Yuanchun Li. Budgetthinker: Empowering budget-aware llm reasoning with control tokens.
 718 *arXiv preprint arXiv:2508.17196*, 2025.

719 Tong Xiao, Xin Xu, Zhenya Huang, Hongyu Gao, Quan Liu, Qi Liu, and Enhong Chen. Advancing
 720 multimodal reasoning capabilities of multimodal large language models via visual perception
 721 reward. *arXiv preprint arXiv:2506.07218*, 2025.

722

723 Xin Xu, Tong Xiao, Zitong Chao, Zhenya Huang, Can Yang, and Yang Wang. Can llms solve longer
 724 math word problems better? *ArXiv preprint*, abs/2405.14804, 2024. URL <https://arxiv.org/abs/2405.14804>.

725

726 Xin Xu, Tianhao Chen, Fan Zhang, Wanlong Liu, Pengxiang Li, Ajay Kumar Jaiswal, Yuchen Yan,
 727 Jishan Hu, Yang Wang, Hao Chen, et al. Double-checker: Enhancing reasoning of slow-thinking
 728 llms via self-critical fine-tuning. *arXiv preprint arXiv:2506.21285*, 2025a.

729

730 Xin Xu, Qiyun Xu, Tong Xiao, Tianhao Chen, Yuchen Yan, Jiaxin Zhang, Shizhe Diao, Can Yang,
 731 and Yang Wang. Ugphysics: A comprehensive benchmark for undergraduate physics reasoning
 732 with large language models. *arXiv preprint arXiv:2502.00334*, 2025b.

733

734 Xin Xu, Jiaxin Zhang, Tianhao Chen, Zitong Chao, Jishan Hu, and Can Yang. Ugmathbench:
 735 A diverse and dynamic benchmark for undergraduate-level mathematical reasoning with large
 736 language models. *arXiv preprint arXiv:2501.13766*, 2025c.

737

738 Zhenghai Xue, Longtao Zheng, Qian Liu, Yingru Li, Zejun Ma, and Bo An. Simpletir: End-to-
 739 end reinforcement learning for multi-turn tool-integrated reasoning. <https://simpletir.notion.site/report>, 2025. Notion Blog.

740

741 An Yang, Beichen Zhang, Binyuan Hui, Bofei Gao, Bowen Yu, Chengpeng Li, Dayiheng Liu, Jian-
 742 hong Tu, Jingren Zhou, Junyang Lin, et al. Qwen2. 5-math technical report: Toward mathematical
 743 expert model via self-improvement. *arXiv preprint arXiv:2409.12122*, 2024.

744

745 An Yang, Anfeng Li, Baosong Yang, Beichen Zhang, Binyuan Hui, Bo Zheng, Bowen Yu,
 746 Chang Gao, Chengan Huang, Chenxu Lv, et al. Qwen3 technical report. *arXiv preprint
 747 arXiv:2505.09388*, 2025a.

748

749 Chenxu Yang, Qingyi Si, Mz Dai, Dingyu Yao, Mingyu Zheng, Minghui Chen, Zheng Lin, and
 750 Weiping Wang. Test-time prompt intervention. *arXiv preprint arXiv:2508.02511*, 2025b.

751

752 Chenxu Yang, Qingyi Si, Yongjie Duan, Zheliang Zhu, Chenyu Zhu, Qiaowei Li, Zheng Lin, Li Cao,
 753 and Weiping Wang. Dynamic early exit in reasoning models. *arXiv preprint arXiv:2504.15895*,
 2025c.

754

755 Yixin Ye, Zhen Huang, Yang Xiao, Ethan Chern, Shijie Xia, and Pengfei Liu. Limo: Less is more
 for reasoning. *arXiv preprint arXiv:2502.03387*, 2025.

756 Longhui Yu, Weisen Jiang, Han Shi, Jincheng Yu, Zhengying Liu, Yu Zhang, James T Kwok,
 757 Zhenguo Li, Adrian Weller, and Weiyang Liu. Metamath: Bootstrap your own mathematical
 758 questions for large language models. *ArXiv preprint*, abs/2309.12284, 2023. URL <https://arxiv.org/abs/2309.12284>.

759

760 Qiyi Yu, Zheng Zhang, Ruofei Zhu, Yufeng Yuan, Xiaochen Zuo, Yu Yue, Weinan Dai, Tiantian
 761 Fan, Gaohong Liu, Lingjun Liu, et al. Dapo: An open-source llm reinforcement learning system
 762 at scale. *arXiv preprint arXiv:2503.14476*, 2025.

763

764 Aohan Zeng, Xin Lv, Qinkai Zheng, Zhenyu Hou, Bin Chen, Chengxing Xie, Cunxiang Wang,
 765 Da Yin, Hao Zeng, Jiajie Zhang, et al. Glm-4.5: Agentic, reasoning, and coding (arc) foundation
 766 models. *arXiv preprint arXiv:2508.06471*, 2025a.

767

768 Weihao Zeng, Yuzhen Huang, Qian Liu, Wei Liu, Keqing He, Zejun Ma, and Junxian He. Simplerl-
 769 zoo: Investigating and taming zero reinforcement learning for open base models in the wild. *arXiv*
 770 *preprint arXiv:2503.18892*, 2025b.

771

772 Fuxiang Zhang, Jiacheng Xu, Chaojie Wang, Ce Cui, Yang Liu, and Bo An. Incentivizing llms to
 773 self-verify their answers. *arXiv preprint arXiv:2506.01369*, 2025a.

774

775 Jiajie Zhang, Nianyi Lin, Lei Hou, Ling Feng, and Juanzi Li. Adaptthink: Reasoning models can
 776 learn when to think. *arXiv preprint arXiv:2505.13417*, 2025b.

777

778 Xiaoying Zhang, Hao Sun, Yipeng Zhang, Kaituo Feng, Chaochao Lu, Chao Yang, and Helen Meng.
 779 Critique-grpo: Advancing llm reasoning with natural language and numerical feedback. *arXiv*
 780 *preprint arXiv:2506.03106*, 2025c.

781

782 Xiaoyun Zhang, Jingqing Ruan, Xing Ma, Yawen Zhu, Haodong Zhao, Hao Li, Jiansong Chen,
 783 Ke Zeng, and Xunliang Cai. When to continue thinking: Adaptive thinking mode switching for
 784 efficient reasoning. *arXiv preprint arXiv:2505.15400*, 2025d.

785

786 Chujie Zheng, Shixuan Liu, Mingze Li, Xiong-Hui Chen, Bowen Yu, Chang Gao, Kai Dang,
 787 Yuqiong Liu, Rui Men, An Yang, et al. Group sequence policy optimization. *arXiv preprint*
 788 *arXiv:2507.18071*, 2025.

789

790

791

792

793

794

795

796

797

798

799

800

801

802

803

804

805

806

807

808

809

810 A BACKGROUND AND PRELIMINARY
811812 A.1 RLVR ALGORITHMS
813814 **Proximal Policy Optimization (PPO).** PPO (Schulman et al., 2017) constrains the policy update
815 within a proximal region of the old policy $\pi_{\theta_{\text{old}}}$ through the clipping mechanism. Specifically, PPO
816 employs the following objective (we omit the KL regularization term hereinafter for brevity):
817

818
$$\mathcal{J}_{\text{PPO}}(\theta) = \mathbb{E}_{x \sim \mathcal{D}, y \sim \pi_{\theta_{\text{old}}}(\cdot | x)} \left[\frac{1}{|y|} \sum_{t=1}^{|y|} \min \left(r_t(\theta) \hat{A}_t, \text{clip} (r_t(\theta), 1 - \varepsilon, 1 + \varepsilon) \hat{A}_t \right) \right], \quad (4)$$

819
820

821 with the importance ratio of the token y_t is defined as $r_t(\theta) = \frac{\pi_{\theta}(y_t | x, y_{<t})}{\pi_{\theta_{\text{old}}}(y_t | x, y_{<t})}$, the advantage \hat{A}_t of y_t
822 is estimated by a value model, and ε is the clipping range of importance ratios.
823824 **Group Relative Policy Optimization (GRPO).** GRPO (Shao et al., 2024) bypasses the need for
825 the value model by computing the relative advantage of each response within a group of responses
826 to the same query. Specifically, GRPO optimizes $\mathcal{J}_{\text{GRPO}}(\theta) = \mathbb{E}_{x \sim \mathcal{D}} [\mathcal{J}_{\text{GRPO}}(\theta, x)]$, where:
827

828
$$\mathcal{J}_{\text{GRPO}}(\theta, x) = \left[\frac{1}{G} \sum_{i=1}^G \frac{1}{|y_i|} \sum_{t=1}^{|y_i|} \min \left(r_{i,t}(\theta) \hat{A}_{i,t}, \text{clip} (r_{i,t}(\theta), 1 - \varepsilon, 1 + \varepsilon) \hat{A}_{i,t} \right) \right]. \quad (5)$$

829

830 Here $\{y_i\}_{i=1}^G \sim \pi_{\theta_{\text{old}}}(\cdot | x)$, G is the number of generated responses to each query x (i.e., the group
831 size), and $r_{i,t}(\theta)$, $\hat{A}_{i,t}$ is computed as in eq. (2).
832833 Numerous variants have been proposed to improve GRPO. For example, DAPO (Yu et al., 2025)
834 introduces token-level normalization and dynamic sampling; Dr GRPO (Liu et al., 2025b) removes
835 length bias to prevent incorrect responses from growing longer over time; and Wang et al. (2025a)
836 train selectively on forking tokens (see also Section 6). Our TFPI is orthogonal to these RLVR algo-
837 rithms. That is to say, any RLVR algorithm can be applied to our proposed TFPI stage. **To isolate**
838 **the effect of RLVR algorithms, we employ DAPO as our RLVR algorithm in all experiments**
839 **for fair comparison.**
840841 A.2 *ThinkingFree* OPERATION
842843 In Section 3.1, we have shown chat templates for both the original query x and its thinking-free
844 version $x' = \text{ThinkingFree}(x)$ for Qwen models. Here, we showcase one additional example under
845 the DeepSeek (Guo et al., 2025) template as below.
846847 **Template 3 (Thinking Mode (DeepSeek))** Please reason step by step, and put your final answer
848 within \boxed{\cdot}. <|User|>{\textbf{question} (x)}<|Assistant|>\n849 **Template 4 (Thinking-Free Mode (DeepSeek))** Please reason step by step, and put your final
850 answer within \boxed{\cdot}. <|User|>{\textbf{question} (x)}<|Assistant|>\n<think>\n</think>852 B META EXPERIMENTS
853854 B.1 TOKEN CONSUMPTION OF *ThinkingFree*
855856 We provide the detailed experimental setup for the meta-experiment in Section 3.1 in this appendix.
857 For DS-1.5B, we use the decoding parameters suggested by Guo et al. (2025) in thinking mode:
858 temperature = 0.6, top- p = 0.95, and top- k = -1. For Qwen3-4B, we adopt the recommended
859 settings from Yang et al. (2025a) in thinking mode: temperature = 0.6, top- p = 0.95, and top- k =
860 20. For *ThinkingFree*, we set temperature = 0.7, top- p = 0.8, and use both top- k = -1 and top- k = 20. The maximum output length is fixed at 32K tokens for both modes. For evaluation, we
861 sample 32 generations per query on AIME 2025 and report the average number of output tokens.
862 The parameters are given in Table 5 and the results are shown in Figure 2 (Left).
863

864 Table 5: Decoding Parameters of Meta-Experiment in Section 3.1
865

	Thinking Mode	Thinking-Free Mode
DS-1.5B	$T = 0.6$, top- $p = 0.95$, and top- $k = -1$	$T = 0.7$, top- $p = 0.8$, and top- $k = 20$
Qwen3-4B	$T = 0.6$, top- $p = 0.95$, and top- $k = 20$	$T = 0.7$, top- $p = 0.8$, and top- $k = 20$

870
871 B.2 DETAILED SETUP OF *ThinkingFree* TRAINING
872873 We provide the detailed experimental setup for the meta-experiment discussed in Section 3.2 in this
874 appendix.875 For training, we use the DAPO (Yu et al., 2025) algorithm, with configurations identical to those
876 in Appendix C.1, except that the maximum output length is set to 4K. For evaluation, we set the
877 maximum output length to 48K and perform testing in thinking mode as described in Template 1.
878 All other evaluation parameters follow Appendix C.3. Note that the initial avg@32 value in Figure 2
879 (Right) is higher than the value reported in (Yang et al., 2025a) (68.2 vs. 65.6), because we adopt
880 the RoPE scaling method described in Polaris (An et al., 2025).
881882 C EXPERIMENTAL DETAILS
883884 In this appendix, we provide the details of our main experiments in Section 4.
885886 C.1 TRAINING DETAILS
887888 We build on the VeRL codebase (Sheng et al., 2024), with the RLVR loss following the DAPO
889 recipe (Yu et al., 2025). Specifically, the RLVR loss is defined in eq. (1). For our TFPI, it becomes
890

891
$$\mathbb{E}_{x \sim \mathcal{D}} [\mathcal{J}_{\text{DAPO}}(\theta, x')], \quad x' = \text{ThinkingFree}(x). \quad (6)$$

892

893 For fair comparison, we use identical hyperparameters across methods. For *clip-higher*, we set
894 $\varepsilon_{\text{low}} = 0.2$ and $\varepsilon_{\text{high}} = 0.28$. Training is performed with a batch size and mini-batch size of 256, a
895 learning rate of 10^{-6} , and no warm-up scheduling. Both KL divergence loss and entropy loss are
896 excluded.897 For rollout, we use temperature = 1, topp = 1, and topk = -1. We generate 8 rollouts per problem.
898 Experiments are conducted on DS-1.5B, Qwen3-4B, and DS-7B, with Polaris-53K (An et al.,
899 2025) as the training dataset. **In principle, we could apply dataset filtering at each training
900 stage to accelerate training An et al. (2025). However, for fairness, we deliberately use the full
901 training set for all experiments.**902 For Direct RLVR, the maximum output length is set to 16K for DS-1.5B and DS-7B, and 32K for
903 Qwen3-4B. For TFPI, we adopt a multi-stage training strategy (An et al., 2025; Luo et al., 2025b):
904905

- DS-1.5B and DS-7B: 2K \rightarrow 4K \rightarrow 8K.
- Qwen3-4B: 4K \rightarrow 8K \rightarrow 16K.

906907 Our experiments are conducted with 32 H20 GPUs. A summary of the number of training steps
908 and training time is provided in Table 6. **To provide a comprehensive view of training compute,
909 we also report the number of processed tokens and the average MFU in Table 7.** Notably, our
910 method achieves a higher MFU and therefore can generate more tokens than “Direct RL” within the
911 same wall-clock time. This arises because shorter responses during RL training reduce rollout-stage
912 “bubble”, yielding a practical efficiency advantage.
913914 C.2 BASELINES
915916 To evaluate the efficacy of TFPI, we compare TFPI with direct RLVR training from an SFT-distilled
917 LRM (“Direct RL” for short) under the same total training compute, i.e., the combined compute of
918 the three TFPI stages equals that of direct RLVR (Table 1). To examine the effect of inserting a TFPI

918 Table 6: Training Steps and Time of Main Experiments. “kh” denotes one thousand H20 Hours.
919

	DS-1.5B	Qwen3-4B	DS-7B	DS-1.5B	Qwen3-4B	DS-7B
TFPI Stage 1	2K, 1K steps	4K, 100 steps	2K, 1K steps	0.84 kh	0.35 kh	1.73 kh
TFPI Stage 2	4K, 440 steps	8K, 56 steps	4K, 232 steps	0.62 kh	0.52 kh	0.82 kh
TFPI Stage 3	8K, 440 steps	16K, 64 steps	8K, 144 steps	1.21 kh	0.91 kh	0.94 kh
TFPI Total	-	-	-	2.66 kh	1.79 kh	3.50 kh
Direct RLVR	16K, 456 steps	32K, 20 steps	16K, 280 steps	2.67 kh	1.9 kh	3.52 kh
TFPI: RLVR	16K, 472 steps	32K, 192 steps	536 steps	2.49 kh	13.5 kh	6.55 kh
TFPI + RLVR Total	-	-	-	5.16 kh	15.4 kh	10 kh
Direct RLVR Total	16K, 896 steps	32K, 216 steps	16K, 820 steps	5.17 kh	15.7 kh	10.1 kh

929 Table 7: Total processed tokens and the average MFU (in %) of Main Experiments.
930

	DS-1.5B	Qwen3-4B	DS-7B	DS-1.5B	Qwen3-4B	DS-7B
TFPI Stage 1	2.37×10^9	5.00×10^8	2.75×10^9	69.27	66.28	73.73
TFPI Stage 2	2.26×10^9	5.02×10^8	1.20×10^9	69.54	66.67	73.79
TFPI Stage 3	3.92×10^9	4.94×10^8	1.24×10^9	68.66	66.76	73.76
TFPI Total	8.55×10^9	1.50×10^9	5.19×10^9	-	-	-
Direct RLVR	7.48×10^9	6.48×10^8	4.77×10^9	68.42	61.57	72.83
TFPI: RLVR	6.26×10^9	5.80×10^9	7.98×10^9	66.20	60.08	72.58
TFPI + RLVR Total	1.48×10^{10}	7.30×10^9	1.27×10^{10}	-	-	-
Direct RLVR Total	1.44×10^{10}	7.36×10^9	1.38×10^{10}	68.11	62.24	72.89

942 stage before RLVR, we apply TFPI to an SFT-distilled model (“TFPI + RL”), continue with standard
943 RLVR, and compare the results with “Direct RL” using approximately the same training compute
944 (Table 2). We also include several high-performing LRM s of the same model size from previous
945 works for reference, including Polaris (An et al., 2025), DeepScaleR (Luo et al., 2025b), Skywork-
946 OR1 (He et al., 2025), and AReal-RL. For both Table 1 and Table 2, all models are evaluated in
947 thinking mode (see also Appendix C.3). To assess the impact of TFPI on reasoning efficiency, we
948 compare our TFPI-trained model with various RL-based efficient reasoning baselines, including
949 TLMRE (Arora & Zanette, 2025), AdaptThink (Zhang et al., 2025b), AutoThink (Tu et al., 2025),
950 Laser (Liu et al., 2025a), L1Max (Aggarwal & Welleck, 2025), and ThinkLess (Fang et al., 2025)
951 (Table 3). The training and testing settings of these baselines, as reported in their original papers,
952 are summarized in Table 8. **For fair comparison, we standardize the testing parameters to $\text{topk} = 0.95$, $\text{topk} = -1$, and $T = 0.6$ with a 32K maximum length**, following the recommendations of
953 DeepSeek-R1 (Guo et al., 2025).
954

955 Table 8: Training and evaluation details of efficient reasoning baselines from original papers. We
956 unify the evaluation setting for fair comparison in Table 3. Details are provided in Appendix C.2
957 and C.3.
958

Model	Training Data	Training Length	Test Length	Evaluation Details
DeepSeek-Distill-Qwen-1.5B				
TLMRE-DS-1.5B ($\alpha = 0.1$)	3.2K examples from NuminaMath	-	32K	10 generations for AIME24
AdaptThink-1.5B ($\delta = 0.05$)	DeepScaleR-40K	16K	16K	$T = 0.6$, 16 generations for AIME24
AutoThink-DS-1.5B-Stage3	DeepScaleR-40K	8K \rightarrow 16K \rightarrow 24K	-	$T = 0.6$, 16 generations
Laser-DE-L4096-1.5B	DeepScaleR-40K	-	32K	16 generations for AIME24
DeepScaleR-1.5B-Preview				
AutoThink-Stage3	DeepScaleR-40K	8K \rightarrow 16K \rightarrow 24K	-	$T = 0.6$, 16 generations
L1-1.5B-Max	DeepScaleR-40K	4K	8K	-
Thinkless-1.5B-RL	DeepScaleR-40K	24K	-	-

968
969 C.3 EVALUATION DETAILS
970971 To comprehensively evaluate model capabilities, we employ a diverse set of benchmarks covering
972 mathematical reasoning, multi-task reasoning, code generation, and instruction-following:

972
973
974
975
976
977
978
979
980
981
982
983
984
985
986
987
988
989
990
991
992
993
994
995
996
997
998
999
1000
1001
1002
1003
1004
1005
1006
1007
1008
1009
1010
1011
1012
1013
1014
1015
1016
1017
1018
1019
1020
1021
1022
1023
1024
1025

- Mathematical reasoning:** We evaluate on AIME24, AIME25, and BeyondAIME (ByteDance-Seed, 2025). For AIME24 and AIME25, we report `pass@1` accuracy using 32 samples per problem (`avg@32`); for BeyondAIME, we report `avg@8`.
- Multi-task reasoning:** We evaluate on GPQA-Diamond (Rein et al., 2024) and report `pass@1` with 8 samples per problem.
- Code generation:** We assess coding ability on LiveCodeBench (Jain et al., 2024) (2024-08-2025-01 subset, aligned with DeepSeek-R1 (Guo et al., 2025)), reporting `pass@1` with 8 samples per problem.
- Instruction-following:** We evaluate on IFEval (Zhou et al., 2023) and report `pass@1` of the strict prompt accuracy with 4 samples per problem.

All evaluation codes are adapted from the DeepscaleR (Luo et al., 2025b) codebase, where vLLM (Kwon et al., 2023) is leveraged to accelerate inference. For IFEval, we use the same codes provided by the official paper (Zhou et al., 2023).

We provide our decoding parameters as follows:

- **Table 1:** We set the temperature to 0.6 and `topp` = 0.95. For LRMAs trained from DS-1.5B and DS-7B, we use `topk` = -1 with a maximum sequence length of 32K tokens. For LRMAs trained from Qwen3-4B, we use `topk` = 20 with a maximum sequence length of 48K tokens, applying RoPE scaling as proposed by An et al. (2025).
- **Table 2:** We set the temperature to 0.6 and `topp` = 0.95. For LRMAs initialized from DS-1.5B and DS-7B, we use `topk` = -1 with a maximum sequence length of 32K tokens. For LRMAs initialized from Qwen3-4B, we use `topk` = 20 with a maximum sequence length of 48K tokens, again applying RoPE scaling as proposed by An et al. (2025). For models marked with “*”, we report the results from their original publications (see Appendix C.4).
- **Table 3:** For efficient reasoning baselines listed in Table 8 and the thinking mode of initial models, we set `topp` = 0.95, `topk` = -1, and $T = 0.6$, with a maximum sequence length of 32K tokens (48K for Qwen3-4B). For the thinking-free mode of initial models and our TFPI, we set `topp` = 0.8, `topk` = 20, and $T = 0.7$ with a maximum sequence length of 32K tokens, following Yang et al. (2025a).

C.4 SOURCE OF SOME RESULTS IN TABLE 2

Results for LRMAs marked with “*” are taken directly from the Seed-1.5-Thinking report (Seed et al., 2025) and the corresponding Hugging Face page of Qwen3-2507. Note that the LiveCodeBench test set subsets of these results, and the metric of IFEval may differ from those in our experiments; their results are included for reference only.

D ANALYSIS DETAILS

As *verification* is an important indicator of slow-thinking capabilities (Setlur et al., 2025), we conduct experiments in Section 5.1 to examine how *verification* can generalize to slow-thinking, even when trained with TFPI (thinking-free mode). Following Yang et al. (2025b), for the experiments in Figure 3, we segmented the reasoning trajectories using ‘\n\n’ as delimiters and classified each step according to whether it contained verification-related phrases such as “wait”, “let me verify”, “let me check”, “checking”, “verifying”, or “double-check”.

E THE USE OF LARGE LANGUAGE MODELS

We only used LLMs (specifically GPT-5) for language refinement during the writing process of this work; all ideas, experimental designs, and analyses were conducted by the authors. The text polished by GPT-5 was subsequently reviewed and verified by us to ensure the quality of the content.

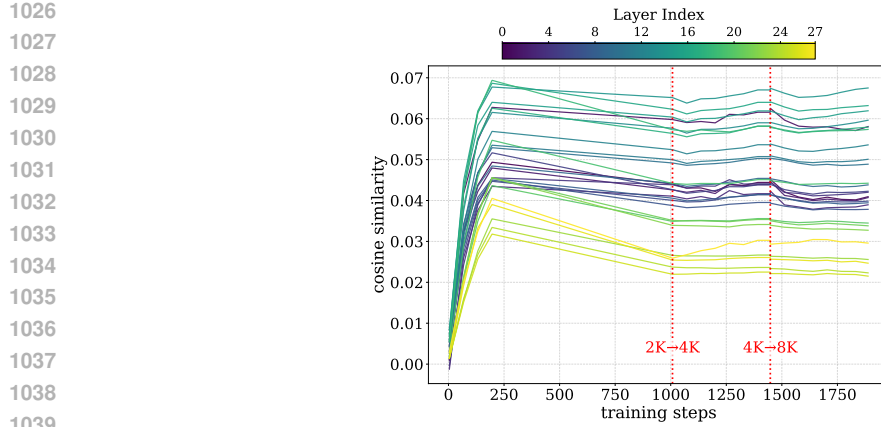


Figure 6: Cosine similarity between parameter updates of TFPI-trained checkpoints and an early “Direct RL” update of DS-1.5B across layers during training.

F MORE RESULTS

F.1 ADDITIONAL RESULTS OF PARAMETER-LEVEL ANALYSIS

Figure 4 (right) reports the cosine similarity of parameter-update vectors between TFPI-trained checkpoints and the final Direct RL checkpoint. For completeness, Figure 6 presents the cosine similarity between TFPI-trained checkpoints and an early Direct RL checkpoint (step 456) from the DS-1.5B run used in Table 1. We observe stronger alignment with the final Direct RL checkpoint than with the early-stage checkpoint.

F.2 COMPLETE RESULTS OF TABLE 2 AND TABLE 3

Due to the page limit, we present only representative results in Sections 4.3 and 4.4, with the complete results provided in Tables 9 and 10, respectively.

F.3 THINKING VS. THINKING-FREE INFERENCE

To compare thinking and thinking-free modes, Table 11 reports accuracy and average output token counts across training stages of TFPI for Qwen3-4B. The accuracy gap between the two modes narrows from Stage 1 to Stage 3. In Stage 3, the thinking mode achieves an average accuracy of 63.9%, whereas the thinking-free mode achieves 60.0%. Meanwhile, the thinking-free mode produces substantially fewer tokens on average (9.9k vs. 15.3k). One may choose the thinking-free mode to trade a modest decrease in accuracy for improved efficiency, or switch between modes to balance accuracy and cost.

F.4 ABOUT DECODING PARAMETERS

The decoding parameters used in our main-text experiments are detailed in Appendices B and C.3. Following the official Hugging Face recommendations for each model, we adopt different settings for the thinking and thinking-free modes. To assess robustness, we additionally report results under a unified configuration: temperature = 0.6, top-p = 0.95, top-k = 20, and a maximum output length of 32k tokens. As shown in Tables 13, 14, 15, and 16, all of our conclusions remain unchanged under this unified setting.

Polaris (An et al., 2025) reports that longer-context inference with RoPE scaling improves performance on harder questions and evaluates at 90K tokens. We find that 90K is prohibitively slow, and 48K suffices based on the clip ratio analysis (Table 12). As shown in Table 15, constraining the maximum output length to 32K slightly degrades the performance of the thinking mode for models RL-tuned from Qwen3-4B. We therefore recommend a 48K context length for Qwen3-4B-based RL-tuned models.

Table 9: Results (%) of RL after TFPI (“TFPI+RL”) vs. “Direct RL” across different benchmarks. “Avg@k” denotes the average accuracy (%) over k random generations (i.e., pass@1). For LRM marked with “*”, results are taken from the corresponding reports (see Appendix C.4); all other results are from our own runs. All models are evaluated in thinking mode. The total training compute for “TFPI+RL” is matched to that of “Direct RL” for fair comparison.

Models	Mathematics			Multi-Task	Code	Instruction	Overall
	AIME 24 Avg@32	AIME 25 Avg@32	Beyond AIME Avg@8	GPQA Avg@8	LiveCode Avg@8	IFEval Avg@4	Overall Avg.
DeepSeek R1*	79.8	65.0	42.4	71.5	64.3	86.1	68.2
Seed-1.5-Thinking*	86.7	74.0	48.0	77.3	64.9	87.4	73.0
Claude4 Opus Thinking*	-	75.5	-	79.6	48.9	89.7	-
Qwen3-235B-Thinking*	85.7	81.5	-	71.1	55.7	83.4	-
Qwen3-8B	75.3	67.0	43.2	61.7	51.7	66.0	61.7
DS-R1-0528-Qwen3-8B	82.8	74.6	50.6	61.4	59.0	73.9	67.0
1.5B Size							
DeepScaleR-1.5B	37.8	31.6	13.1	19.1	21.9	40.5	27.3
DS-1.5B Direct RL	37.2	28.5	12.9	24.6	19.5	39.5	27.0
DS-1.5B TFPI stage 3	40.1	30.8	13.8	29.6	19.9	40.8	29.2
DS-1.5B TFPI + RL	42.3	32.9	15.1	27.8	20.9	41.0	30.0
4B Size							
Polaris-4B-Preview	73.2	70.7	39.9	54.9	39.7	63.9	57.0
Qwen3-4B Direct RL	78.8	71.5	46.4	56.2	54.3	65.1	62.0
Qwen3-4B TFPI stage 3	79.9	70.6	46.7	58.5	57.0	70.2	63.8
Qwen3-4B TFPI + RL	80.8	76.0	49.5	61.1	55.7	71.3	65.7
Qwen3-4B-2507-Thinking - TFPI only	84.7	79.2	51.5	66.4	62.4	68.0	68.7
7B Size							
ARReal-boba-RL-7B	61.5	46.1	30.7	35.4	34.2	57.5	44.2
Skywork-OR1-7B-Preview	61.2	46.4	31.2	35.2	43.3	55.4	45.5
Polaris-7B-Preview	70.6	48.8	37.0	34.1	43.9	55.6	48.3
DS-7B Direct RL	62.3	47.9	30.1	36.9	42.8	57.1	46.2
DS-7B TFPI stage 3	62.0	44.6	31.1	46.8	42.1	60.2	47.8
DS-7B TFPI + RL	65.3	47.1	33.2	45.9	43.3	57.3	48.7

Table 10: Comparison of the Thinking-Free inference mode of TFPI with efficient reasoning baselines across various reasoning tasks. “Avg@k” denotes the average accuracy (in %) over k generations (i.e., pass@1), and “Toks” indicates the average output length in thousands of tokens (K).

Models	AIME 24		AIME 25		Beyond AIME		GPQA		Overall	
	avg@32	Toks	avg@32	Toks	avg@8	Toks	avg@8	Toks	Avg.	Toks
DeepSeek-Distill-Qwen-1.5B										
TLMRE-DS-1.5B ($\alpha = 0.1$)	27.6	12.9	24.8	12.5	9.2	11.9	14.8	7.5	19.1	11.2
AdaptThink-1.5B ($\delta = 0.05$)	28.1	8.0	22.6	7.9	10.0	4.8	14.8	5.1	18.9	6.5
AutoThink-DS-1.5B-Stage3	30.3	10.2	25.2	9.1	9.4	8.7	17.4	7.0	20.6	8.7
Laser-DE-L4096-1.5B	30.3	8.3	24.9	7.4	9.7	7.4	21.1	4.7	21.5	6.9
Initial Model (Thinking)	29.6	16.7	23.0	16.5	8.7	14.4	16.3	9.8	19.4	14.3
Initial Model (Thinking-Free)	12.4	5.7	10.9	4.4	4.4	3.4	4.2	0.9	8.0	3.6
- TFPI stage 1	21.9	1.6	15.3	1.4	8.7	1.3	32.9	0.8	19.7	1.3
- TFPI stage 2	31.5	3.4	24.2	3.1	10.1	2.9	35.3	1.6	25.3	2.7
- TFPI stage 3	37.5	5.3	28.4	5.0	12.4	4.9	35.6	2.6	28.5	4.4
DeepscaleR-1.5B-Preview										
AutoThink-Stage3	38.9	8.7	28.9	7.7	11.6	7.8	27.3	5.4	26.7	7.4
L1-1.5B-Max	27.2	3.2	26.3	2.9	9.1	3.1	32.4	2.3	23.8	2.9
Thinkless-1.5B-RL	28.4	11.3	24.1	11.1	8.1	11.7	20.3	12.7	20.2	11.7
Qwen3-4B										
Initial Model (Thinking)	73.6	18.0	68.3	22.3	43.4	23.5	56.8	10.7	60.5	18.6
Initial Model (Thinking-Free)	26.9	7.2	20.2	5.5	11.0	4.2	45.0	2.3	25.8	4.8
- TFPI stage 1	43.9	3.7	31.1	3.4	23.2	3.4	47.8	1.5	36.5	3.0
- TFPI stage 2	63.7	7.2	52.8	8.0	33.0	7.0	50.9	2.3	50.1	6.1
- TFPI stage 3	75.1	10.5	66.9	12.7	42.1	12.7	55.9	3.7	60.0	9.9
Qwen3-4B-Instruct-2507	60.4	7.9	46.1	7.4	33.0	7.3	64.4	4.8	51.0	6.9

Table 11: Comparison of the Thinking-Free inference mode with the Thinking mode across various reasoning tasks after TFPI. “Avg@k” denotes the average accuracy (in %) over k generations (i.e., pass@1), and “Toks” indicates the average output length in thousands of tokens (K).

Models	AIME 24		AIME 25		Beyond AIME		GPQA		Overall	
	avg@32	Toks	avg@32	Toks	avg@8	Toks	avg@8	Toks	Avg.	Toks
Qwen3-4B										
Initial Model (Thinking)	73.6	18.0	68.3	22.3	43.4	23.5	56.8	10.7	60.5	18.6
Initial Model (Thinking-Free)	26.9	7.2	20.2	5.5	11.0	4.2	45.0	2.3	25.8	4.8
- TFPI stage 1 (Thinking)	75.2	13.8	67.8	17.1	42.4	16.8	57.9	7.5	60.8	13.8
- TFPI stage 1 (Thinking-Free)	43.9	3.7	31.1	3.4	23.2	3.4	47.8	1.5	36.5	3.0
- TFPI stage 2 (Thinking)	76.0	13.4	68.2	17.0	44.7	16.7	57.8	7.7	61.7	13.7
- TFPI stage 2	63.7	7.2	52.8	8.0	33.0	7.0	50.9	2.3	50.1	6.1
- TFPI stage 3 (Thinking)	79.9	15.1	70.6	18.7	46.7	18.8	58.5	8.6	63.9	15.3
- TFPI stage 3	75.1	10.5	66.9	12.7	42.1	12.7	55.9	3.7	60.0	9.9
Qwen3-4B-Instruct-2507	60.4	7.9	46.1	7.4	33.0	7.3	64.4	4.8	51.0	6.9
Response Length		16K	32K	48K	64K	80K	90K			
Avg@32		42.6	64.1	68.3	68.5	68.5	68.5			
Clip Ratio		55.7	25.7	5.2	1.2	0.6	0.0			

Table 12: AIME25 results for Qwen3-4B: Avg@32 and clip ratio across maximum output lengths.

F.5 ABOUT TRAINING TEMPERATURE

In our main experiments, we set the training temperature to 1.0 (Appendix C.1). Motivated by Polaris (An et al., 2025), which reports an “optimal” temperature of 1.4 for Qwen3-4B, we conduct an ablation on training temperature using Qwen3-4B. As shown in Figure 7, performance at 1.4 is comparable to 1.0 for both TFPI Stage 1 and Direct RL (measured by AVG@32 on AIME25), suggesting that our results are robust to this choice of training temperature.

F.6 ABOUT THE STAGE BOUNDARY AND STAGE LENGTH

Following prior multi-stage training practice (An et al., 2025; Luo et al., 2025b), we increase the training context length when the clip ratio shows a renewed inflection and validation performance begins to plateau. Figure 8 illustrates this behavior for TFPI Stage 1 on Qwen3-4B; step 100 is a natural transition point.

Training context length trades off training throughput and effective learning signal: longer contexts slow training, whereas shorter contexts constrain learning on harder questions. We therefore begin with a shorter length and expand as training stabilizes. To set stage lengths, we prioritize effective signal: with 8-sample rollouts, 0/8 or 8/8 correctness contributes no learning signal (Yu et al., 2025), so for a candidate length L , we compute the share of questions with 1/8–7/8 correctness as a proxy for effective training mass. We choose L to preserve throughput while maintaining substantial effective mass at each stage. For Qwen3–4B, $L=4K$ yields 28K/53K questions in the 1/8–7/8 band, whereas $L=8K$ yields 29K/53K; thus we start at 4K for efficiency and move to 8K once validation gains plateau. Note that the effective sets across stages are not disjoint; for instance, the same ques-

Table 13: Re-evaluate the meta-experiment in Figure 2 (Left) under a unified evaluation setting (temperature = 0.6, top-p = 0.95, top-k = 20). “# Tokens” denotes the average number of tokens on AIM25 and “ Δ ” is the percentage of reduction in token consumption.

Model	# Tokens (Thinking)	# Tokens (Thinking-Free)	Δ
DS-1.5B (original setting)	16.5K	4.4K	-73%
Unified Setting	16.4K	3.6K	-78%
Qwen3-4B (original setting)	17.4K	5.1K	-71%
Unified Setting	17.4K	4.7K	-73%

Table 14: Results of TFPI vs. direct RL across different benchmarks. “Avg@k” denotes the average accuracy (%) over k random generations (i.e., pass@1). All models are evaluated in thinking mode. The total training compute for the 3 stages of TFPI equals that of “Direct RL” for fair comparison. This table corresponds to Table 1 under a unified decoding setting.

Models	Mathematics			Multi-Task	Code	Instruction	Overall
	AIME 24 Avg@32	AIME 25 Avg@32	Beyond AIME Avg@8	GPQA Avg@8	LiveCode Avg@8	IFEval Avg@4	Overall Avg.
DeepSeek-Distill-Qwen-1.5B							
Initial Model	29.1	25.5	9.0	16.3	17.6	40.1	22.9
- Direct RL	35.5	27.9	12.5	20.2	18.7	38.1	25.5
- TFPI stage 1	31.8	26.7	12.5	30	18.9	39.5	26.6
- TFPI stage 2	35.1	27.6	13.4	29.7	18.9	44.0	28.1
- TFPI stage 3	36.1	30.1	14.9	28.5	21.0	41.8	28.7
Qwen3-4B							
Initial Model	71.6	64.1	41.5	56.6	54.9	64.9	58.9
Direct RL	73.4	62.2	41.1	56.2	52.1	66.0	58.5
TFPI stage 1	74.7	67.4	42.1	57.9	55.3	66.0	60.6
TFPI stage 2	75.6	67.5	44.6	57.8	54.6	64.8	60.8
TFPI stage 3	78.7	69.5	46.1	58.5	56.8	70.2	63.3
DeepSeek-Distill-Qwen-7B							
Initial Model	53.3	40.5	25.0	36.8	37.6	55.6	41.5
- Direct RL	56.8	41.6	26.7	37.4	39.6	58.2	43.4
- TFPI stage 1	58.8	39.6	28.8	49.4	40.1	56.6	45.5
- TFPI stage 2	61.7	42.9	31.5	47.5	42.0	57.5	47.2
- TFPI stage 3	62.6	43.2	30.7	47.1	42.4	59.3	47.5

Table 15: Results (%) of RL after TFPI (“TFPI+RL”) vs. “Direct RL” across different benchmarks. “Avg@k” denotes the average accuracy (%) over k random generations (i.e., pass@1). For LRM marked with “*”, results are taken from the corresponding reports (see Appendix C.4); All models are evaluated in thinking mode. The total training compute for “TFPI+RL” is matched to that of “Direct RL” for fair comparison. This table corresponds to Table 2 under a unified decoding setting.

Models	Mathematics			Multi-Task	Code	Instruction	Overall
	AIME 24 Avg@32	AIME 25 Avg@32	Beyond AIME Avg@8	GPQA Avg@8	LiveCode Avg@8	IFEval Avg@4	Overall Avg.
DeepSeek R1*	79.8	65.0	42.4	71.5	64.3	86.1	68.2
Seed-1.5-Thinking*	86.7	74.0	48.0	77.3	64.9	87.4	73.0
Claude4 Opus Thinking*	-	75.5	-	79.6	48.9	89.7	-
Qwen3-235B-Thinking*	85.7	81.5	-	71.1	55.7	83.4	-
Qwen3-4B Direct RL	75.8	65.8	42.1	56.0	53.9	65.1	59.8
Qwen3-4B TFPI stage 3	78.7	69.5	46.1	58.5	56.8	70.2	63.3
Qwen3-4B TFPI + RL	77.9	70.8	47.5	60.8	54.5	71.3	63.8

tion may score 3/8 at 4K and 6/8 at 8K. In all experiments, we train on the full Polaris-53K dataset to ensure fairness. However, for better efficiency, one can curate stage-specific subsets based on the effective-signal criterion by filtering out questions that are 0/8 or 8/8 correct under the current context length.

F.7 MULTI-STAGE DIRECT RL (4K → 8K → 16K)

Figure 2 (right) shows that applying Direct RL with a 4K response length causes a substantial performance drop on AIME25 for Qwen3-4B. In contrast, TFPI trains stably even at 4K, suggesting that—even in a multi-stage setting—the initial stage length should not be too short. We posit that enabling multi-stage training with short response lengths is a key benefit of TFPI. To rule out the possibility that this effect is an artifact of staging, we run Direct RL with the identical multi-stage schedule on Qwen3-4B. The complete results are reported in Table 17, with training details provided in Table 18.

Table 16: Comparison of the Thinking-Free inference mode of TFPI with efficient reasoning baselines across various reasoning tasks. “Avg@k” denotes the average accuracy (in %) over k generations (i.e., pass@1), and “Toks” indicates the average output length in thousands of tokens (K). Models with “*” are trained from DeepScaleR-1.5B, while the remaining are from DS-1.5B. This table corresponds to Table 3 under a unified decoding setting.

Models	AIME 24		AIME 25		Beyond AIME		GPQA		Overall	
	avg@32	Toks	avg@32	Toks	avg@8	Toks	avg@8	Toks	Avg.	Toks
1) TLMRE-DS-1.5B ($\alpha = 0.1$)	27.6	12.9	24.8	12.5	9.2	11.9	14.8	7.5	19.1	11.2
2) AdaptThink-1.5B ($\delta = 0.05$)	28.1	8.0	22.6	7.9	10.0	4.8	14.8	5.1	18.9	6.5
3) AutoThink-DS-1.5B-Stage3	30.3	10.2	25.2	9.1	9.4	8.7	17.4	7.0	20.6	8.7
4) Laser-DE-L4096-1.5B	30.3	8.3	24.9	7.4	9.7	7.4	21.1	4.7	21.5	6.9
5) AutoThink-Stage3*	38.9	8.7	28.9	7.7	11.6	7.8	27.3	5.4	26.7	7.4
6) L1-1.5B-Max*	27.2	3.2	26.3	2.9	9.1	3.1	32.4	2.3	23.8	2.9
7) Thinkless-1.5B-RL*	28.4	11.3	24.1	11.1	8.1	11.7	20.3	12.7	20.2	11.7
DS-1.5B (Thinking)	29.1	16.5	25.5	16.4	9.0	17.3	16.3	9.8	20.0	15.0
DS-1.5B (Thinking-Free)	13.3	5.1	11.0	3.6	4.0	2.6	6.2	0.9	8.6	3.0
- TFPI stage 1	23.9	1.5	16.2	1.4	9.1	1.2	36.4	0.8	21.4	1.2
- TFPI stage 2	28.6	3.4	25.0	3.0	10.6	2.9	35.7	1.6	25.0	2.7
- TFPI stage 3	37.7	5.2	28.4	5.1	14.5	4.9	34.1	2.6	28.7	4.4

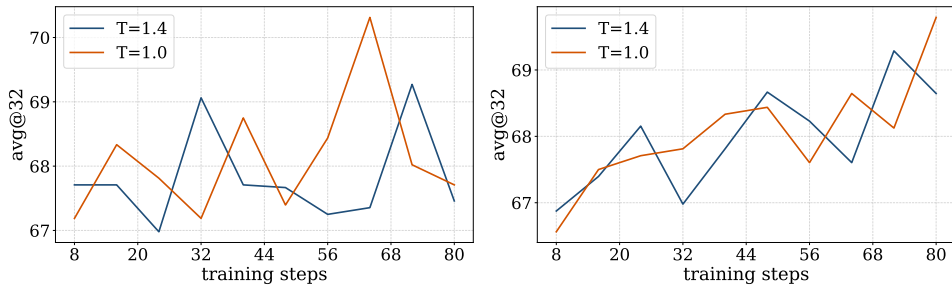


Figure 7: Avg@32 (%) on AIME25 for Qwen3-4B across training steps under different training temperatures (1.4 vs. 1.0). Left: Stage 1 of TFPI; Right: Direct RL.

Table 17: TFPI v.s. Multi-Stage Direct RL. All models are evaluated in thinking mode.

Models	Mathematics			Multi-Task		Code		Instruction		Overall
	AIME 24 Avg@32	AIME 25 Avg@32	Beyond AIME Avg@8	GPQA Avg@8	LiveCode Avg@8	IFEval Avg@4	Overall Avg.			
Initial Model	73.6	68.3	43.4	56.8	54.9	64.9	60.3			
TFPI stage 1	75.2	67.8	42.4	57.9	55.3	66.0	60.8			
Multi-Stage Direct RL Stage 1	49.2	36.0	22.6	51.4	44.0	64.5	44.6			
TFPI stage 2	76.0	68.2	44.7	57.8	54.8	64.8	61.0			
Multi-Stage Direct RL Stage 2	58.4	42.3	28.2	52.9	48.4	63.2	48.9			
TFPI stage 3	79.9	70.6	46.7	58.5	57.0	70.2	63.8			
Multi-Stage Direct RL Stage 3	64.9	48.6	32.5	55.2	51.0	65.2	52.9			

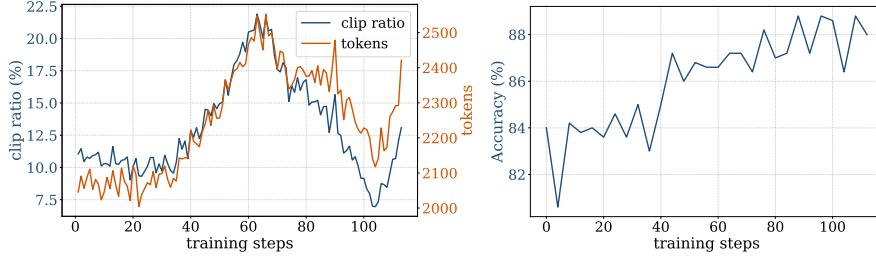


Figure 8: Qwen3-4B TFPI Stage 1. Left: clip ratio and average output tokens over training steps; Right: MATH500 validation accuracy. Step 100 marks a turning point.

1296 Table 18: Training Steps, Time, and MFU of TFPI v.s. Direct RL with Qwen3-4B.
1297

	Training Steps	Training Time (kh)	MFU (%)
TFPI Stage 1	4K, 100 steps	0.35	66.28
Multi-Stage Direct RL Stage 1	4K, 100 steps	0.45	66.82
TFPI Stage 2	8K, 56 steps	0.52	66.67
Multi-Stage Direct RL Stage 2	8K, 56 steps	0.51	66.31
TFPI Stage 3	16K, 64 steps	0.91	66.76
Multi-Stage Direct RL Stage 3	16K, 64 steps	0.97	65.99
TFPI Total	-	1.79	-
Multi-Stage Direct RL Total	-	1.93	-

1309
1310 **G REPRODUCIBILITY STATEMENT**
1311

1312 To ensure reproducibility, we provide a detailed description of our method in Section 3.3 and present
 1313 all experimental setups in Section 4.1 and Appendix C, including training configurations and eval-
 1314 uation protocols. All evaluation datasets, the training set, the training framework, testing codes, as
 1315 well as the efficient reasoning baselines used in our experiments, are publicly available and prop-
 1316 erly referenced (see Appendix C). We will also release our codes and training checkpoints upon
 1317 acceptance for reproducibility.

1318
1319
1320
1321
1322
1323
1324
1325
1326
1327
1328
1329
1330
1331
1332
1333
1334
1335
1336
1337
1338
1339
1340
1341
1342
1343
1344
1345
1346
1347
1348
1349